~~RESTRICTED~~

Copy No. 11

RM No. A7K24

NACA RM No. A7K24

A 7 K 24

6179

TECH LIBRARY KAFB, NM

0069289

RESEARCH MEMORANDUM

WIND-TUNNEL INVESTIGATION OF HORIZONTAL TAILS.

I - UNSWEPT AND 35° SWEPT-BACK PLAN FORMS OF ASPECT RATIO 3

By Jules B. Dods, Jr.

Ames Aeronautical Laboratory
Moffett Field, Calif.

Declassified by Authority of LaRC Security Classification Office (Sec) Letter dated June 16, 1983
Marvin Johnson

AFMDC
TECHNICAL LIBRARY
AFL 2611

This document contains classified information affecting the National Defense of the United States within the meaning of the Espionage Act, USC 50:31 and 32. Its transmission or the revelation of its contents in any manner to an unauthorized person is prohibited by law. Information so classified may be imparted only to persons in the military and naval services of the United States, appropriate civilian officers and employees of the Federal Government who have a legitimate interest therein and to United States citizens of known loyalty and discretion who of necessity must be informed thereof.

NATIONAL ADVISORY COMMITTEE
FOR AERONAUTICS

WASHINGTON

April 22, 1948

~~RESTRICTED~~

219.98/13

National Aeronautics and
Space Administration

Langley Research Center
Hampton, Virginia
23665

NASA

Reply to Attn of 139A

JUN 1 6 1983

TO: Distribution

FROM: 180A/Security Classification Officer

SUBJECT: Authority to Declassify NACA/NASA Documents Dated Prior to January 1, 1960

Effective this date, all material (informal, correspondence) classified by this Center prior to January 1, 1960, is declassified. This action does not include material derivatively classified at the Center upon instructions from other Agencies.

Immediate re-marking is not required; however, until material is re-marked by lining through the classification and annotating with the following statement, it must continue to be protected as if classified:

> "Declassified by authority of LaRC Security Classification Officer (SCO) letter dated June 16, 1983," and the signature of person performing the re-marking.

If re-marking a large amount of material is desirable, but unduly burdensome, custodians may follow the instructions contained in NHB 1640.4, subpart F, section 1203.604, paragraph (h).

This declassification action complements earlier actions by the National Archives and Records Service (NARS) and by the NASA Security Classification Officer (SCO). In Declassification Review Program 807008, NARS declassified the Center's "Research Authorization" files, which contain reports, Research Authorizations, correspondence, photographs, and other documentation. Earlier, in a 1971 letter, the NASA SCO declassified all NACA/NASA formal series documents with the exception of the following reports, which must remain classified:

Document No.	First Author
E-51A30	Nagey
E-53G20	Francisco
E-53G21	Johnson
E-53K18	Spooner
SL-54J21a	Westphal
E-55C16	Fox
E-56H23a	Himmel

JUN 2 3 1983

05-05-1997 11:29 804 864 2375 LARC TECH LIBRARY P.02

If you have any questions concerning this matter, please call Mr. William L. Simkins at extension 3281.

Jess G. Ross
2898

Distribution:
SDL 031

cc:
NASA Scientific and Technical
Information Facility
P.O. Box 8757
BWI Airport, MD 21240

NASA--NIS-5/Security
180A/RIAD
139A/TU&AO
139A/WLSimkins:elf 06/15/83 (3281)
6-15-83
139A/JS 6-15-83

31-01 HEADS OF ORGANIZATIONS
MESS, JANE S.,
MAIL STOP 185 BLDG 1194

05-05-1997 11:29 804 864 2275 LARC TECH LIBRARY P.03

TECH LIBRARY KAFB, NM
0069289

NACA RM No. A7K24 RESTRICTED

NATIONAL ADVISORY COMMITTEE FOR AERONAUTICS

RESEARCH MEMORANDUM

WIND-TUNNEL INVESTIGATION OF HORIZONTAL TAILS. I - UNSWEPT AND 35° SWEPT-BACK PLAN FORMS OF ASPECT RATIO 3.

By Jules B. Dods, Jr.

SUMMARY

The results are presented of a wind-tunnel investigation of the low-speed characteristics of horizontal tails of aspect ratio 3 with unswept and swept-back plan forms. Two models were tested which had identical areas, aspect ratio, taper ratio, and airfoil section, differing only in the angle of sweepback and elevator area ratios. Data are presented for Reynolds numbers of 3.0×10^6 and 4.0×10^6 with the elevator sealed and for a Reynolds number of 3.0×10^6 with the seal removed and with standard roughness applied to the leading edge.

The major effect of sweepback, as measured from the tests of the two models, was to increase the rate of change of hinge-moment coefficient with angle of attack, to reduce the rate of change with elevator deflection, and to reduce the elevator effectiveness.

INTRODUCTION

An investigation of the theoretical prediction of control-surface hinge moments by lifting-surface theory has been undertaken by the NACA. The lifting-surface theory is a further refinement to the lifting-line theory to obtain more accurate predictions. This report presents the experimental results obtained on the first two of a series of models to determine the validity of the theoretical computations and the extent of aspect ratios over which they are valid. The comparisons with the theoretical calculations are not presented herein but will await the results of tests of models of aspect ratios 4.5 and 6.

RESTRICTED

Another equally important purpose of the investigation was to evaluate the effects of sweepback by a comparison of the results of tests of two models with the same area, aspect ratio, taper ratio, and airfoil section, differing mainly in the angle of sweepback.

The present investigation included the measurement of the lift, hinge-moment, and pitching-moment coefficients, and the pressure coefficients across the elevator nose seal of the semispan horizontal tails of unswept and swept-back plan forms and an aspect ratio of 3. The effects of Reynolds number, standard roughness on the leading edge, and removal of the elevator seal were also determined.

The NACA 64A010 airfoil section was chosen for the models. The aft 30 percent of this section is straight sided, thus simplifying control construction and balance.

MODELS

The two models tested in this investigation were of aspect ratio 3, taper ratio 0.5, and the 0.25 chord lines were swept back 11.3° for the unswept model, and 35° for the swept-back model, as shown in figure 1.

The airfoil section was the NACA 64A010 perpendicular to the 0.70-chord line for the unswept plan form and perpendicular to the 0.25-chord line for the swept-back plan form. The airfoil coordinates are presented in table I. The values listed as model coordinates were used for the models, since the true coordinates were not available at the time of model construction. Slight discrepancies between the model and the true coordinates are apparent, but they are not large enough to produce an appreciable effect upon the data.

Both models were equipped with sealed radius-nose elevators. For the unswept tail the elevator chord was 0.30 of the total chord measured perpendicular to the 0.70-chord line. The elevator chord of the swept-back tail was also 0.30 of the total chord; however, the chord was measured perpendicular to the 0.25-chord line as indicated in figure 1(b). In maintaining the same elevator chord ratio along the airfoil section line, the area ratios were of necessity different — 30 percent for the unswept model and 25.6 percent for the swept-back model.

The tip shape for both models was formed by rotating the tip airfoil section parallel to the undisturbed air stream about a line inboard of the tip a distance equal to the maximum tip ordinate, necessitating a short fairing of the tip nose into the leading edge.

Photographs showing the models mounted in the wind tunnel are given in figures 2 and 3. The location of the balance-chamber tubes is given in table II.

COEFFICIENTS AND SYMBOLS

The coefficients and symbols as used throughout the report are defined as follows:

C_L	lift coefficient (L/qS)
C_{h_e}	elevator hinge-moment coefficient $(H/qS_e\bar{c}_e)$ (See appendix)
C_m	pitching-moment coefficient $(M/qS(M.A.C.))$
$\Delta p/q$	pressure coefficient across elevator nose seal (pressure below seal minus pressure above seal divided by the dynamic pressure)
A	aspect ratio $(2b^2/S)$
α	corrected angle of attack, degrees
b	span of the semispan models measured perpendicular to plane of symmetry
b'	span of the elevator measured along the hinge line, feet
$\bar{c}_e$	root-mean-square elevator chord aft of hinge line parallel to the plane of symmetry, feet
$\bar{c}_e'$	root-mean-square elevator chord aft of hinge line perpendicular to the hinge line, feet
δ_e	elevator deflection (positive when trailing edge of elevator is down, measured in a plane normal to the hinge line), degrees
H	hinge moment, foot-pounds

L lift, pounds

M pitching moment about the 0.25 M.A.C., foot-pounds

M_A first moment of the elevator area aft of the hinge line about the hinge line, cubic feet

M.A.C. mean aerodynamic chord, feet

q free-stream dynamic pressure $(\frac{1}{2}\rho V^2)$, pounds per square foot

R Reynolds number $\left[\frac{\rho V(\text{M.A.C.})}{\mu}\right]$

ρ density of air, slugs per cubic foot

μ absolute viscosity in poises

V velocity of air, feet per second

S area of semispan horizontal tail, square feet

S_e area of elevator aft of hinge line, square feet

In addition, the following symbols are used:

$C_{L_\alpha} = (\partial C_L/\partial\alpha)_{\delta_e = 0}$ (measured through $\alpha = 0$)

$C_{L_\delta} = (\partial C_L/\partial\delta_e)_{\alpha = 0}$ (measured through $\delta_e = 0$)

$C_{h_\alpha} = (\partial C_h/\partial\alpha)_{\delta_e = 0}$ (measured through $\alpha = 0$)

$C_{h_\delta} = (\partial C_h/\partial\delta_e)_{\alpha = 0}$ (measured through $\delta_e = 0$)

$\alpha_\delta = -(C_{L_\delta}/C_{L_\alpha})$ (elevator effectiveness parameter)

TESTS

The models were mounted on a turntable flush with the floor of an Ames Aeronautical Laboratory 7- by 10-foot wind tunnel. (See figs. 2 and 3.) Tests were conducted at dynamic pressures of 40 and 80 pounds per square foot, corresponding to Reynolds numbers of 3.0×10^6 and 4.0×10^6, respectively. Standard leading-edge roughness was applied in the manner described in reference 1. Elevator hinge moments were measured by a resistance-type torsional strain gage.

All coefficients and the angle of attack have been corrected for the effects of the tunnel walls. No additional tunnel-wall corrections due to sweepback have been applied.

RESULTS AND DISCUSSION

The data for the unswept tail are presented in figures 4 to 9 and those for the swept-back tail are presented in figures 10 to 15. The variation of lift, hinge-moment, and pitching-moment coefficients with angle of attack are given in figures 4 and 10. Hinge-moment coefficients are also shown as a function of the elevator angle for various angles of attack in figures 5 and 11. In addition, the variation of the pressure coefficient across the elevator nose seal as a function of the angle of attack is presented in figures 6 and 12.

Scale Effect

Data for both the unswept and the swept-back models were obtained at a Reynolds number of 4.0×10^6. The complete results are not presented because the aerodynamic coefficients did not vary significantly from those obtained at a Reynolds number of 3.0×10^6, as illustrated in the comparisons presented in figures 7 and 13. Because of the rather sudden stall of the unswept model it was deemed inadvisable (from structural considerations) to stall the model at the higher Reynolds number. A slight decrease of the maximum lift coefficient was noted for the swept-back plan form with increasing Reynolds number at zero elevator deflection. The lift-curve slope C_{L_α} remained unchanged for both values of the Reynolds number for both tails.

It is noted in figure 4(a) that a different type of stall was measured for the unswept model at positive and negative angles of attack, an unexpected result because the airfoil section was symmetrical. The reason for this difference was investigated, and the only apparent explanation was that the tests were conducted in a critical Reynolds number range for this airfoil section. This contention is partially substantiated by the effect of roughness on the stall in the positive direction as shown in figure 8.

Effect of Standard Roughness

The effect of standard leading-edge roughness upon the lift and hinge-moment coefficients is shown in figure 8 for the unswept tail and in figure 14 for the swept-back tail. In general, little effect was found. The maximum lift of the unswept tail was reduced, but the maximum lift of the swept-back tail remained the same. The effect on the hinge-moment coefficients of the swept-back tail was more pronounced than the effect measured on the unswept tail. No significant change in C_{h_α} was found for either tail.

Effect of Removing Elevator Seal

As would be expected for a nose-radius elevator, the change in the lift and hinge-moment coefficients caused by removal of the elevator seal was small for low elevator deflections and increased for the higher deflections. This is shown in figures 9 and 15.

Pitching Moments

The pitching moments measured about the one-quarter M.A.C. indicate a stabilizing effect of sweepback. The unswept model was slightly unstable statically while the swept-back model was neutrally stable. As the elevator was deflected upward (as in landings or pull-ups) the stability of both tails was increased. (See figs. 4(c) and 10(c)). At the stall, the static longitudinal stability of both models increased markedly, as would be predicted by the results of reference 2.

Effectiveness and Hinge-Moment Parameters

The lift-effectiveness and hinge-moment parameters C_{L_α}, C_{L_δ}, α_δ, C_{h_α}, and C_{h_δ} are listed in table III for the two tails at a Reynolds number of 3.0×10^6. The incremental changes due to Reynolds number, standard roughness, and removal of the elevator seal as discussed in the previous sections are presented for easy reference. As shown in this table, the change in C_{h_α} between the unswept and the swept-back models was from -0.0010 to -0.0013, the change in C_{h_δ} was from -0.0087 to -0.0069, and the tail-effectiveness parameter α_δ was changed from -0.71 to -0.53. The value of C_{L_δ} was reduced by 0.0094, but the slope of the lift curve remained unchanged. As pointed out in a previous section the elevator area

ratios differed between the two models. Although the major part of the changes in the parameters can be attributed to sweepback, the possibility of area ratio effects should be noted.

CONCLUSIONS

The results of tests conducted to determine the low-speed aerodynamic characteristics of horizontal tails of aspect ratio 3.0, of unswept and swept-back plan forms, indicate that:

1. No appreciable scale effect was encountered with or without sweepback for Reynolds numbers from 3.0×10^6 to 4.0×10^6.

2. The effect of standard leading-edge roughness was small with or without sweepback.

3. Removal of the elevator seal did not affect C_{h_α} for either the unswept or the swept-back model.

4. The tail-effectiveness parameter α_δ was changed from −0.71 for the unswept model to −0.53 for the swept-back model.

5. The change in C_{h_α} between the unswept and the swept-back models was from −0.0010 to −0.0013, and C_{h_δ} was changed from −0.0087 to −0.0069.

Ames Aeronautical Laboratory,
National Advisory Committee for Aeronautics,
Moffett Field, Calif.

APPENDIX

Conversion Factors For Hinge-Moment Coefficients

Because several methods are in use for the reduction of hinge moments to coefficient form, particularly for swept-back lifting surfaces, conversion factors for the various methods are presented. To obtain the hinge-moment coefficients for one of the listed methods, multiply the value of the hinge-moment coefficient of this report by the corresponding conversion factor in the following table:

Method of computing hinge-moment coefficients	Unswept tail		Swept-back tail	
	Feet^3	Conversion factor	Feet^3	Conversion factor
$C_{h_e} = \frac{H}{qS_e\bar{c}_e}$	2.395	1.000	1.745	1.000
$C_{h_e} = \frac{H}{qbc_e^2}$	2.439	0.982	1.776	0.982
$C_{h_e} = \frac{H}{qb'\bar{c}_e'^2}$	2.439	.982	1.585	1.101
$C_{h_e} = \frac{H}{2qM_A}$	2.439	.982	1.585	1.101

NACA

REFERENCES

1. Abbott, Ira H., von Doenhoff, Albert E., and Stivers, Louis S., Jr.: Summary of Airfoil Data. NACA ACR No. L5C05, 1945.

2. Shortal, Joseph A., and Maggin, Bernard: Effect of Sweepback and Aspect Ratio on Longitudinal Stability Characteristics of Wings at Low Speeds. NACA TN No. 1093, 1946.

TABLE I

COORDINATES FOR THE NACA 64A010 AIRFOIL

[All Dimensions in Percent of Wing Chord]

Upper and lower surfaces		
Station	NACA 64A010 ordinate	Model ordinate
0	0	0
0.50	0.804	0.819
.75	.969	.987
1.25	1.225	1.247
2.50	1.688	1.696
5.00	2.327	2.333
7.50	2.805	2.780
10.00	3.199	3.202
15.00	3.813	3.816
20.00	4.272	4.280
25.00	4.606	4.610
30.00	4.837	4.842
35.00	4.968	4.950
40.00	4.995	4.975
45.00	4.894	4.889
50.00	4.684	4.672
55.00	4.388	4.373
60.00	4.021	4.011
65.00	3.597	3.594
70.00	3.127	3.131
75.00	2.623	2.637
80.00	2.103	2.120
85.00	1.582	1.595
90.00	1.062	1.071
95.00	.541	.553
100.00	.021	0
L.E. Radius 0.687[1]: T.E. Radius 0.023[1]		

[1]Same for model ordinates.

TABLE II

LOCATION OF THE PRESSURE TUBES IN THE BALANCE CHAMBER IN PERCENT OF THE SEMISPAN

Station	Unswept plan form	Swept-back plan form
1	21.2	15.3
2	42.4	45.0
3	63.7	77.1
4	91.2	92.1

TABLE III

EFFECT OF SCALE, STANDARD LEADING-EDGE ROUGHNESS, AND ELEVATOR NOSE SEAL ON THE EFFECTIVENESS AND HINGE-MOMENT PARAMETERS OF THE UNSWEPT AND SWEPT-BACK PLAN FORMS

Parameter	$R = 3.0 \times 10^6$	Increment due to increasing R to 4.0×10^6	Increment due to roughness on leading edge	Increment due to removing elevator nose seal
Unswept plan form				
c_{h_α}	−0.0010	0.0001	0.0002	0
c_{h_δ}	−.0087	−.0001	0	−0.0003
c_{L_δ}	.0370	−.0018	−.0005	−.0039
α_δ	−.71	.02	.01	.07
c_{L_α}	.053	0	0	0
Swept-back plan form				
c_{h_α}	−0.0013	0.0001	0	0.0001
c_{h_δ}	−.0069	.0003	0.0007	0
c_{L_δ}	.0276	.0004	−.0011	−.0026
α_δ	−.53	0	.02	−.01
c_{L_α}	.053	0	−.001	−.001

NACA

	Unswept	Swept-back
Aspect ratio	3	3
Taper ratio	0.5	0.5
Area semispan	10.083 ft.^{2}	10.083 ft.^{2}
Elevator area	3.024 ft.^{2}	2.581 ft.^{2}
C_e	0.792 ft.	0.676 ft.
M.A.C.	2.688 ft.	2.688 ft

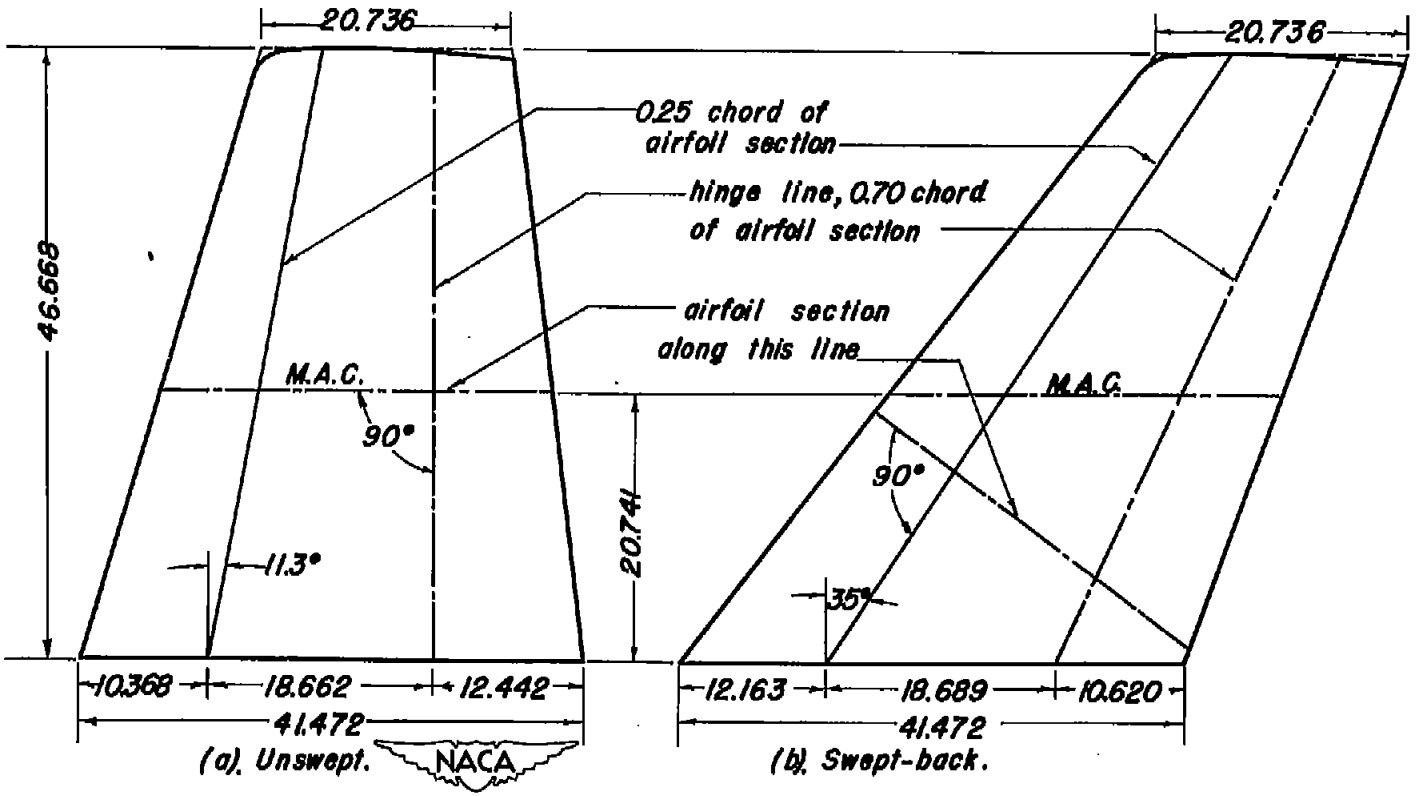

Figure 1.- Plan forms of the horizontal tail models of aspect ratio 3.

(a) Three-quarter front view.

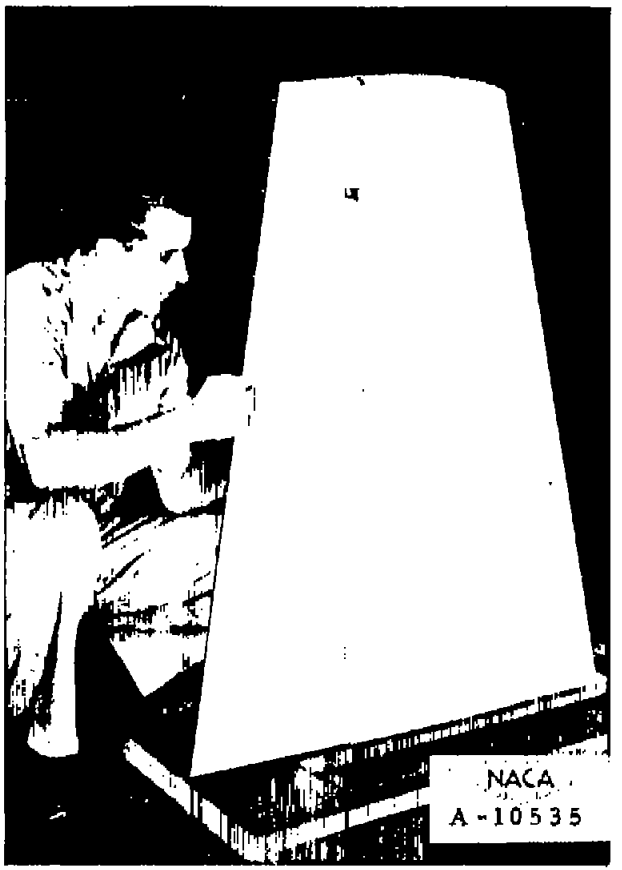

(b) Three-quarter rear view.

Figure 2.- The unswept tail mounted in the 7- by 10-foot wind tunnel.

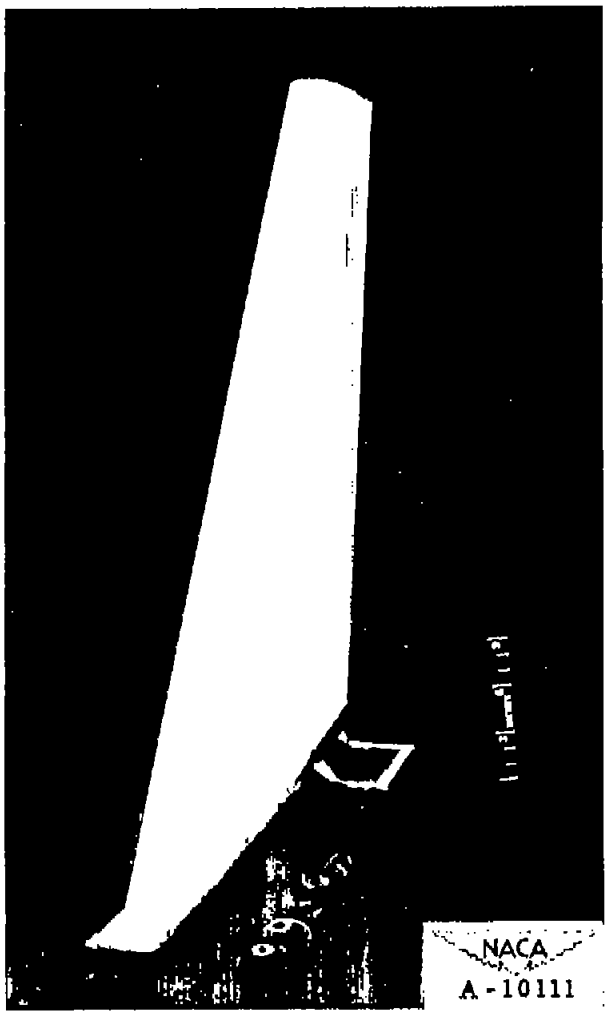

(a) Three-quarter front view.

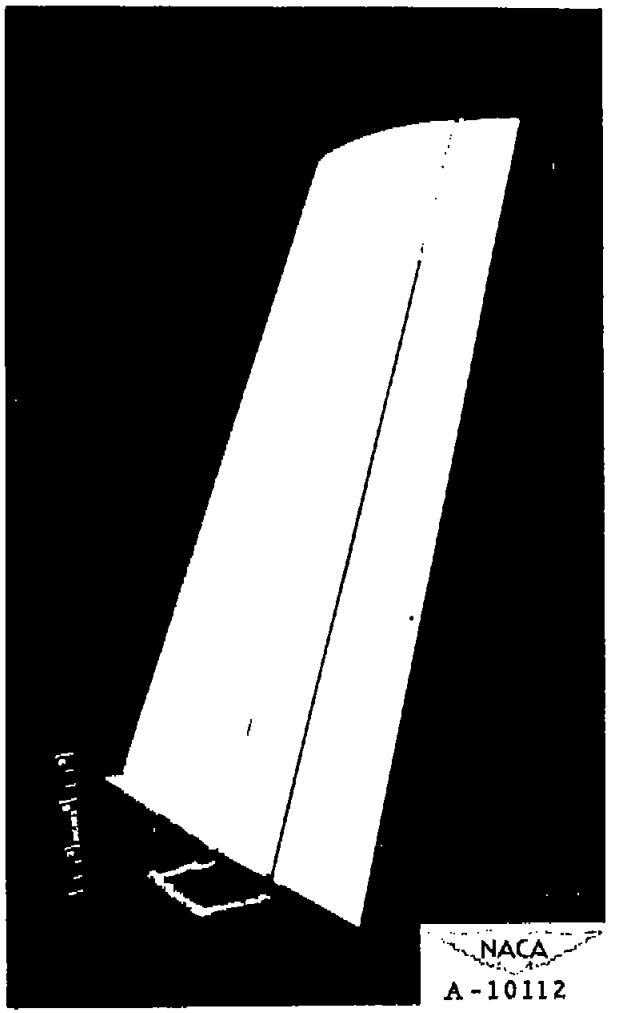

(b) Three-quarter rear view.

Figure 3.- The 35° swept-back tail mounted in the 7- by 10-foot wind tunnel.

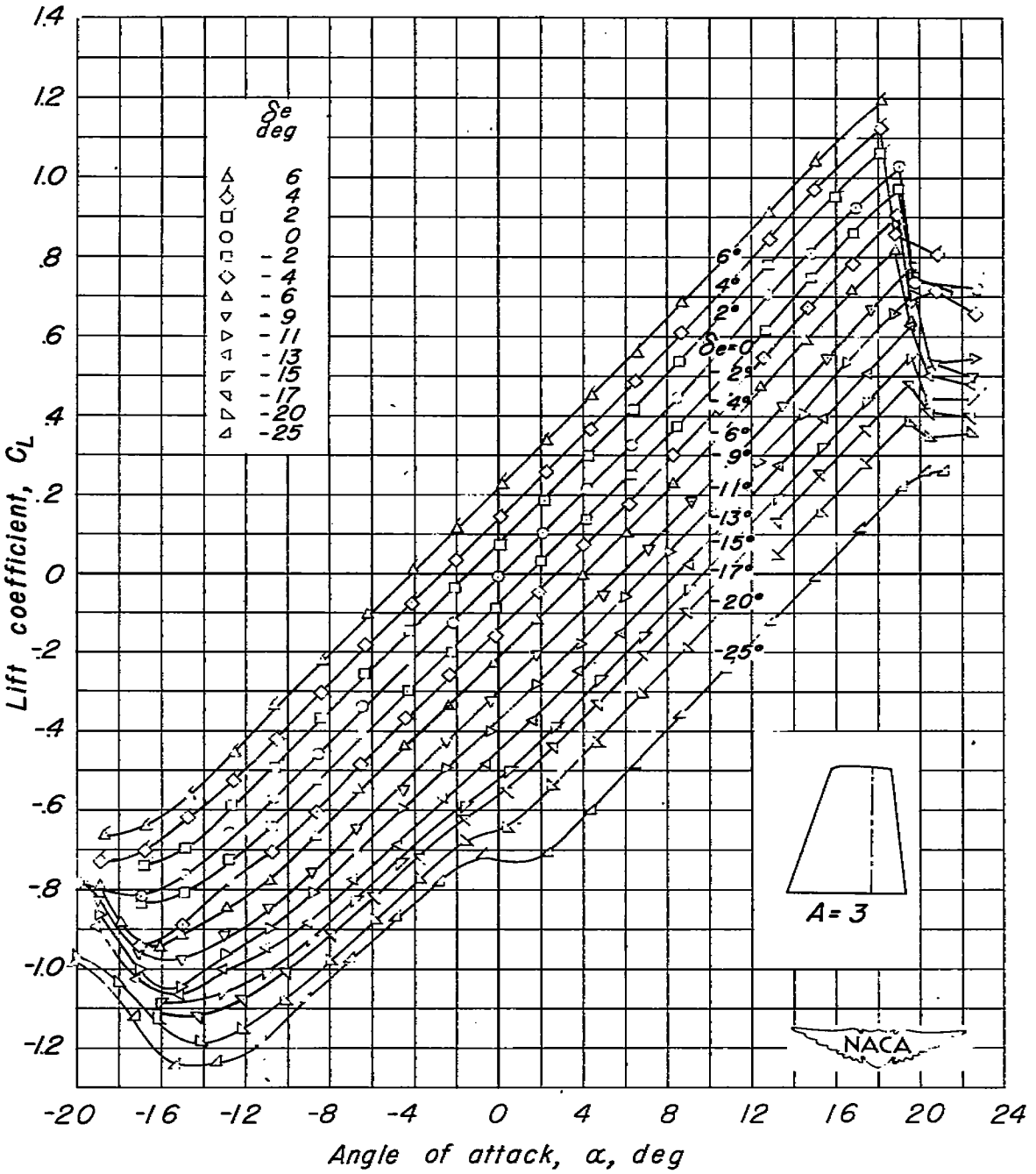

(a) Lift coefficient.

Figure 4.- Lift, hinge-moment, and pitching-moment coefficients of the unswept tail. Aspect ratio 3.0; R, 3.0 x 10^6.

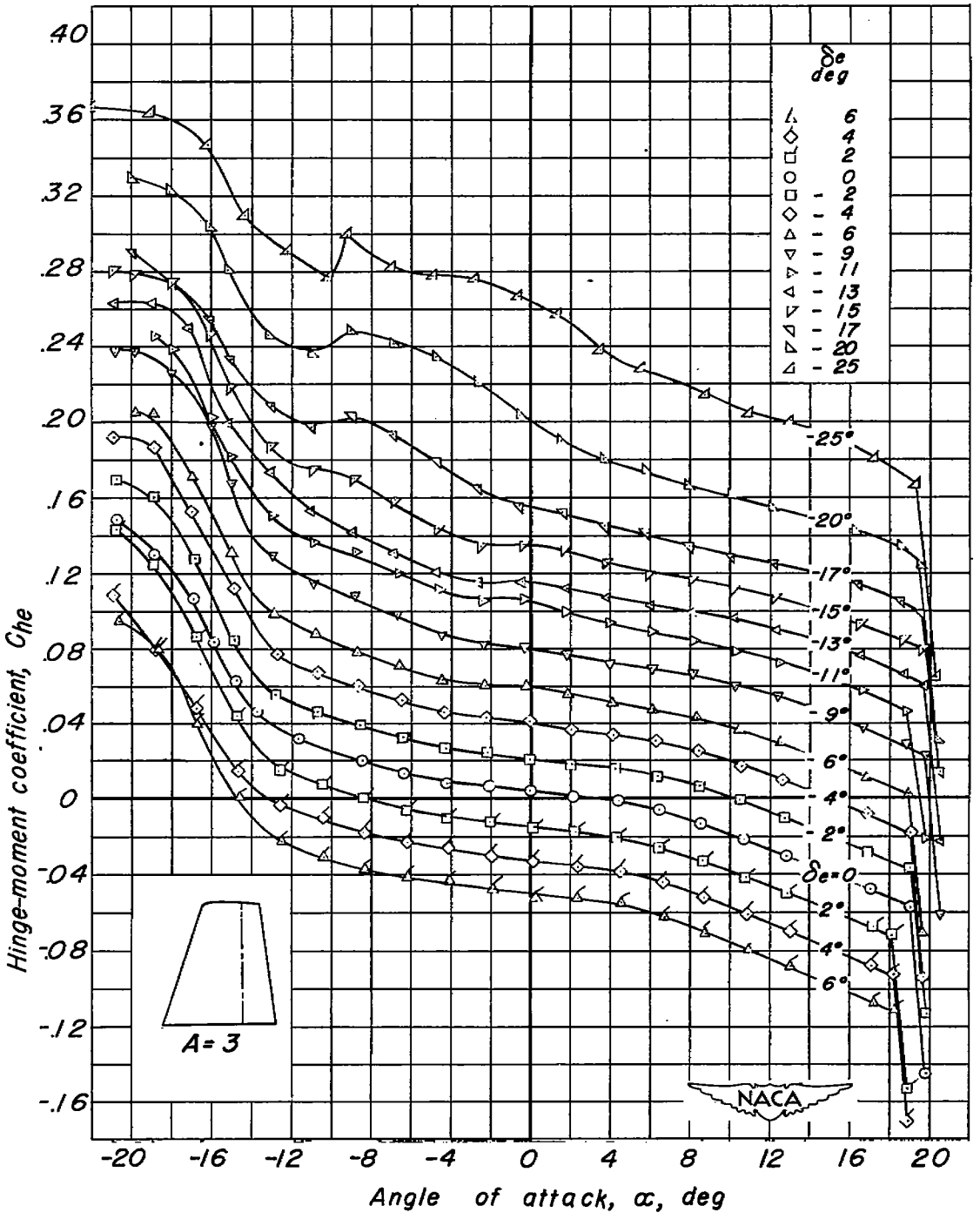

(b) Hinge-moment coefficient.

Figure 4.—continued.

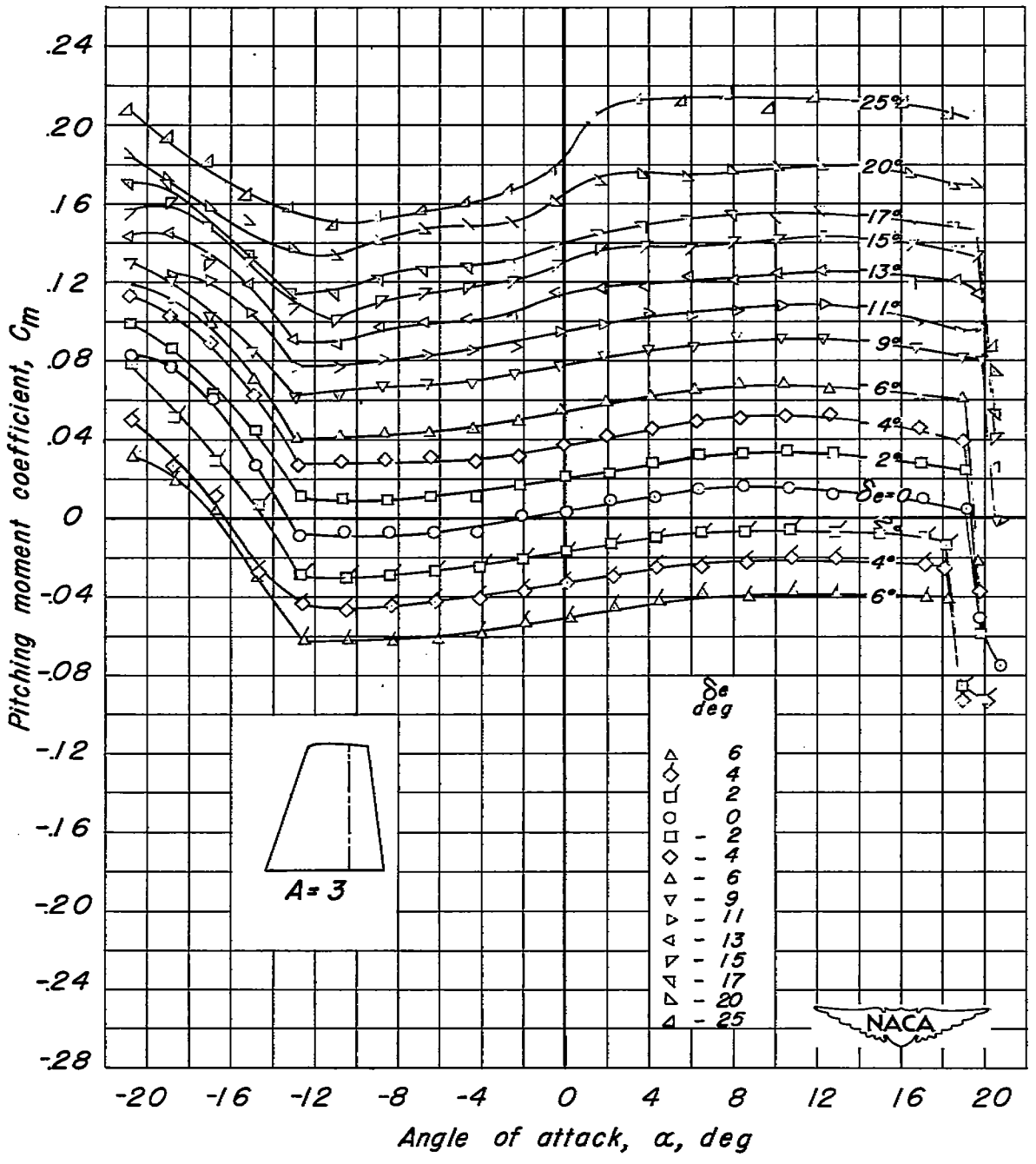

(c) Pitching moment coefficient.

Figure. 4. —concluded.

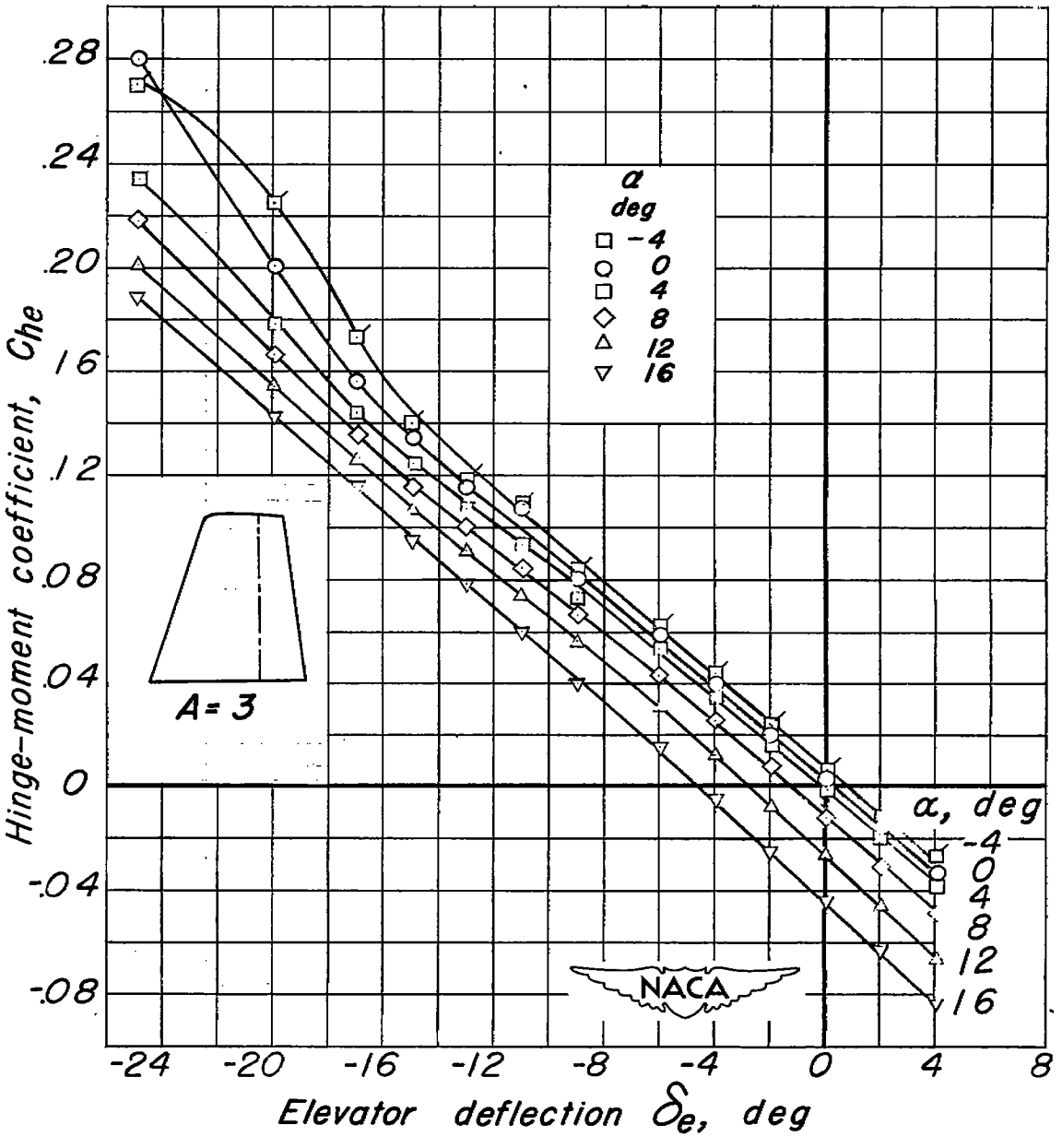

Figure 5.- Variation of hinge-moment coefficient with elevator deflection for various angles of attack of the unswept tail. Aspect ratio, 3; R, 3.0 x 10⁶.

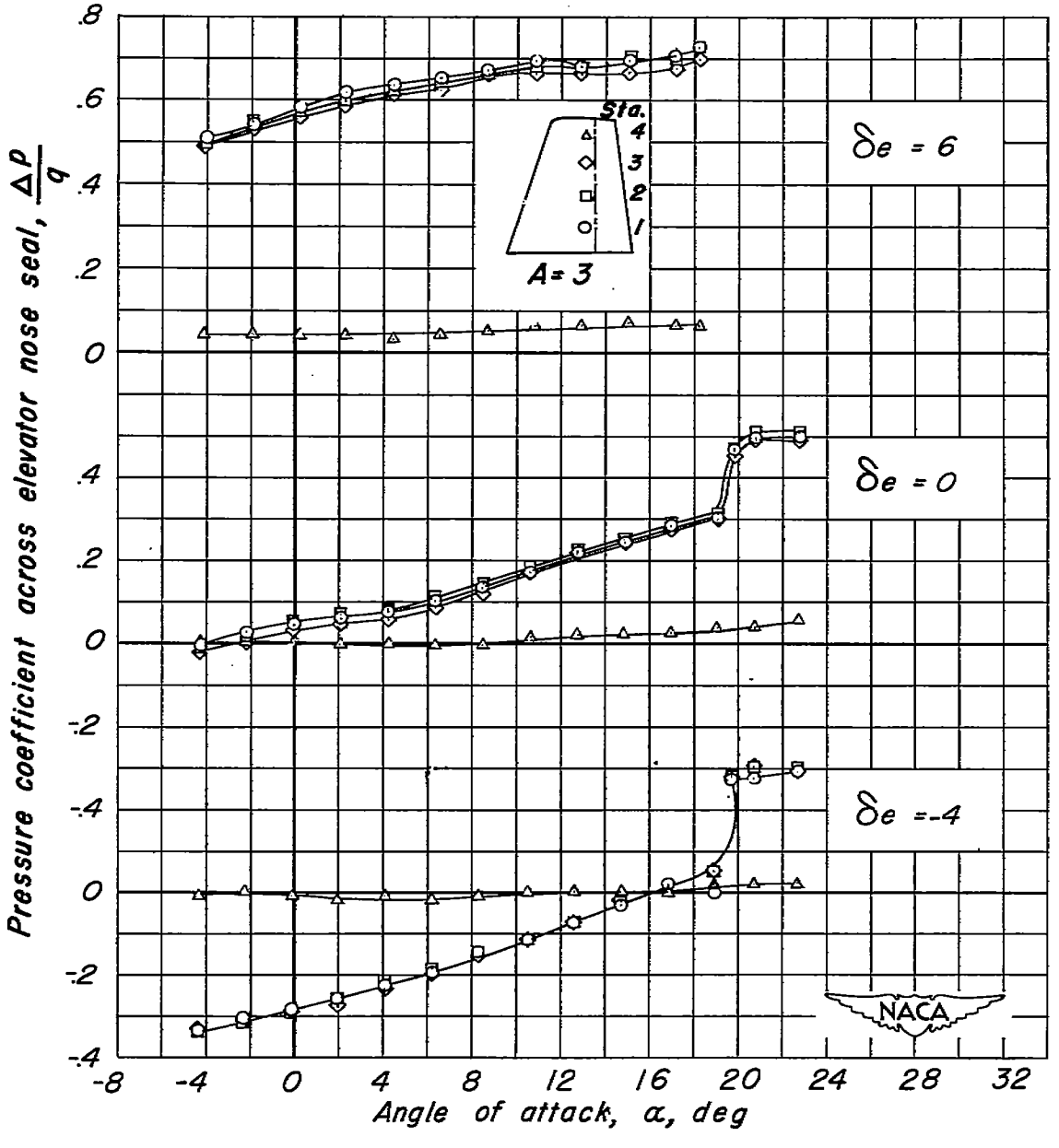

(a) $\delta_e = 6, 0, -4$.

Figure 6.- Variation of pressure coefficient across elevator nose seal with angle of attack of the unswept tail. Aspect ratio 3; R, 3.0 x 10⁶.

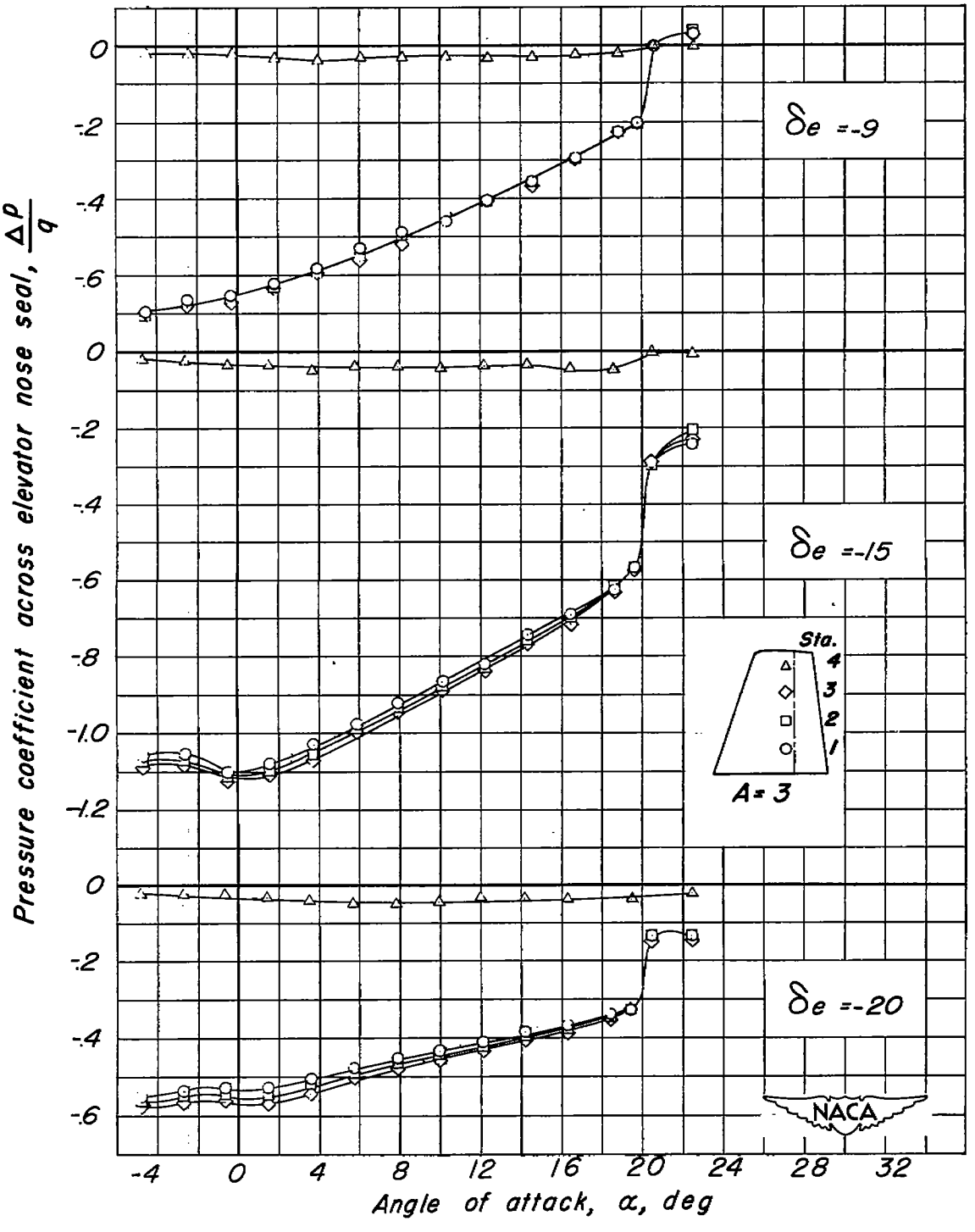

(b) δ_e = -9, -15, -20.

Figure 6. —concluded.

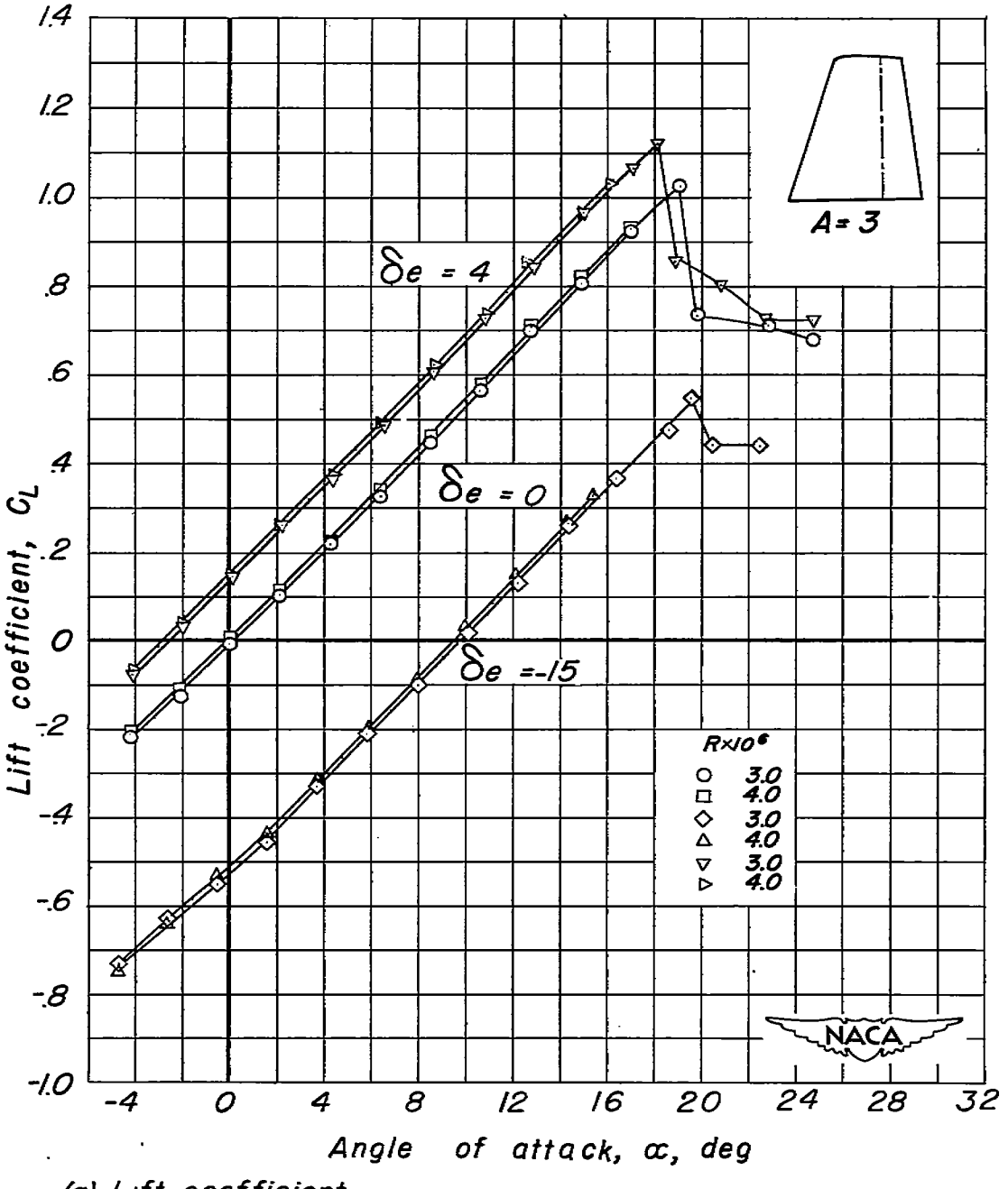

(a) Lift coefficient.

Figure 7.- Comparison of the lift and hinge-moment coefficients at R= 3.0 x 10⁶ and 4.0 x 10⁶ for the unswept tail. Aspect ratio 3.0.

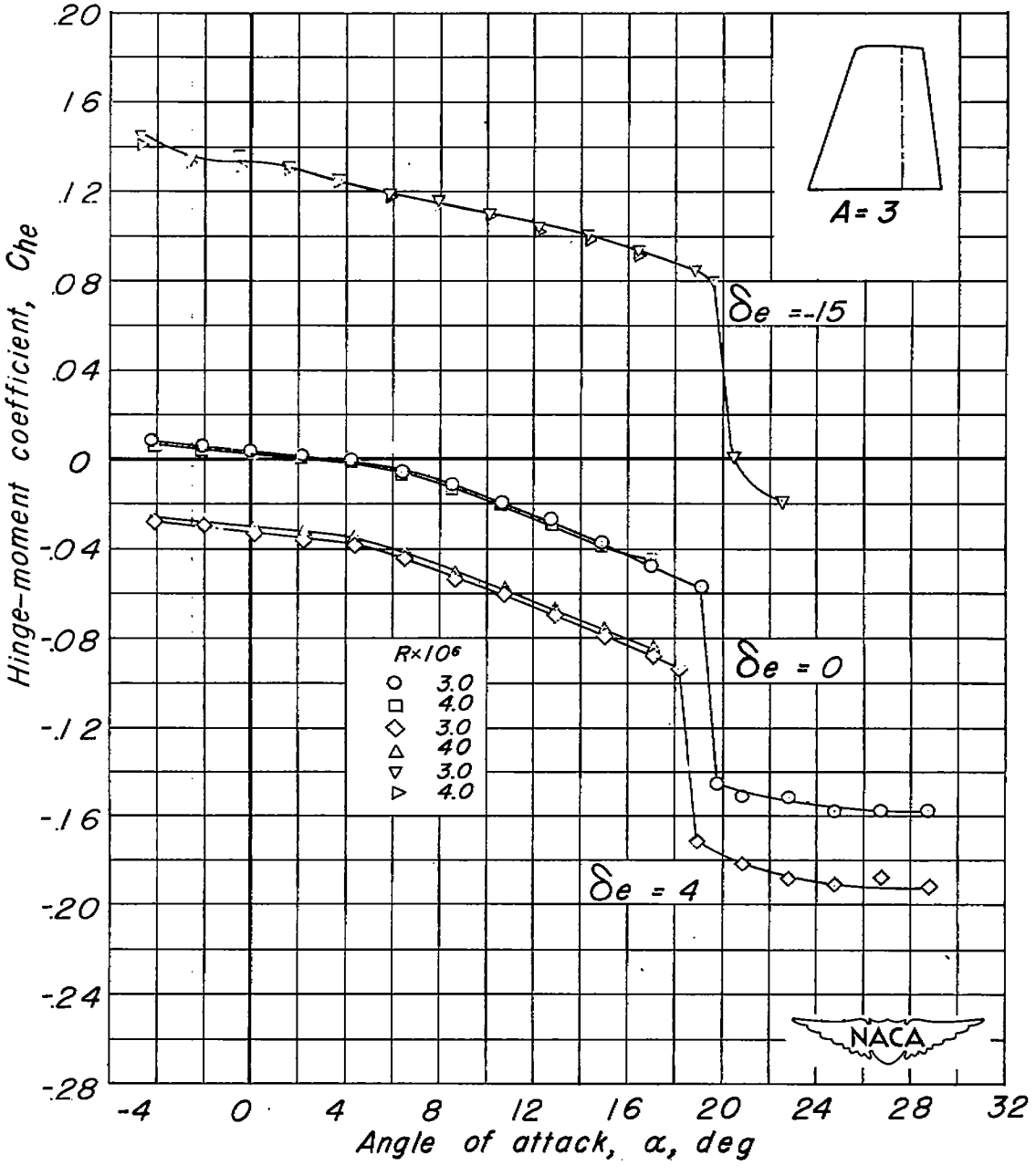

(b) Hinge-moment coefficient.

Figure. 7. —concluded.

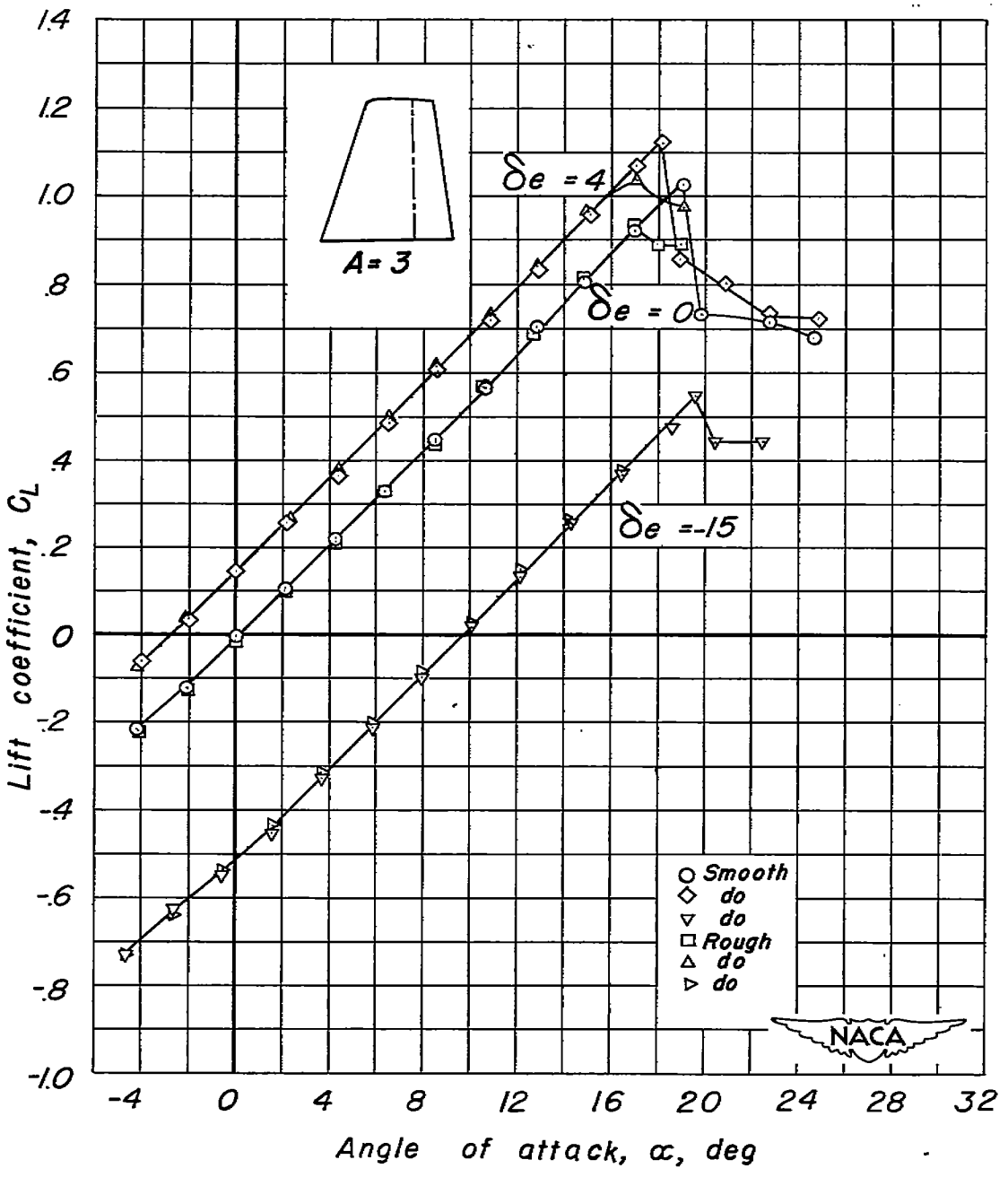

(a) Lift coefficient.

Figure 8.- Comparison of the lift and hinge-moment coefficients of the smooth and rough unswept tail. Aspect ratio 3.0.

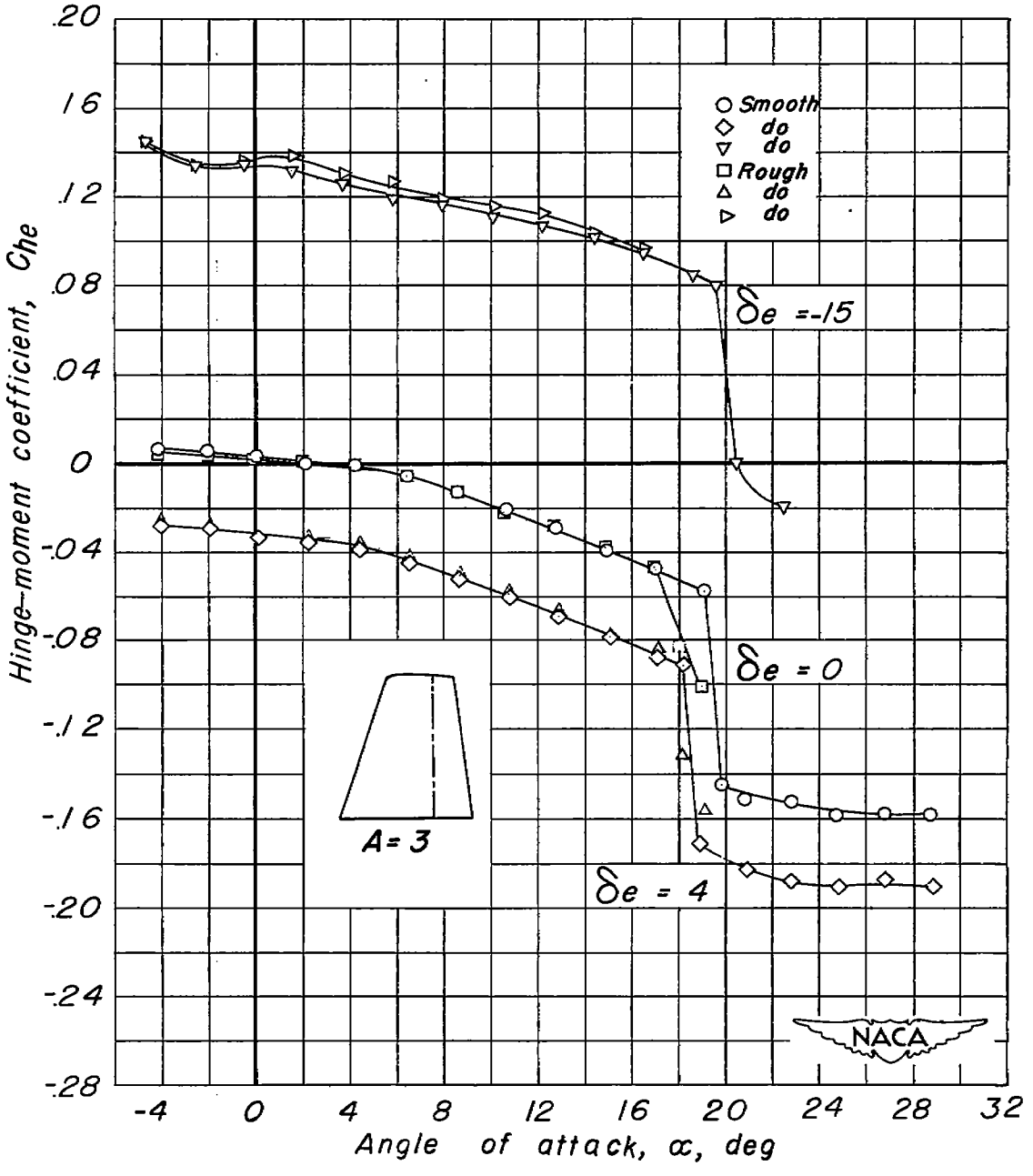

(b) Hinge-moment coefficient.

Figure. 8. —concluded.

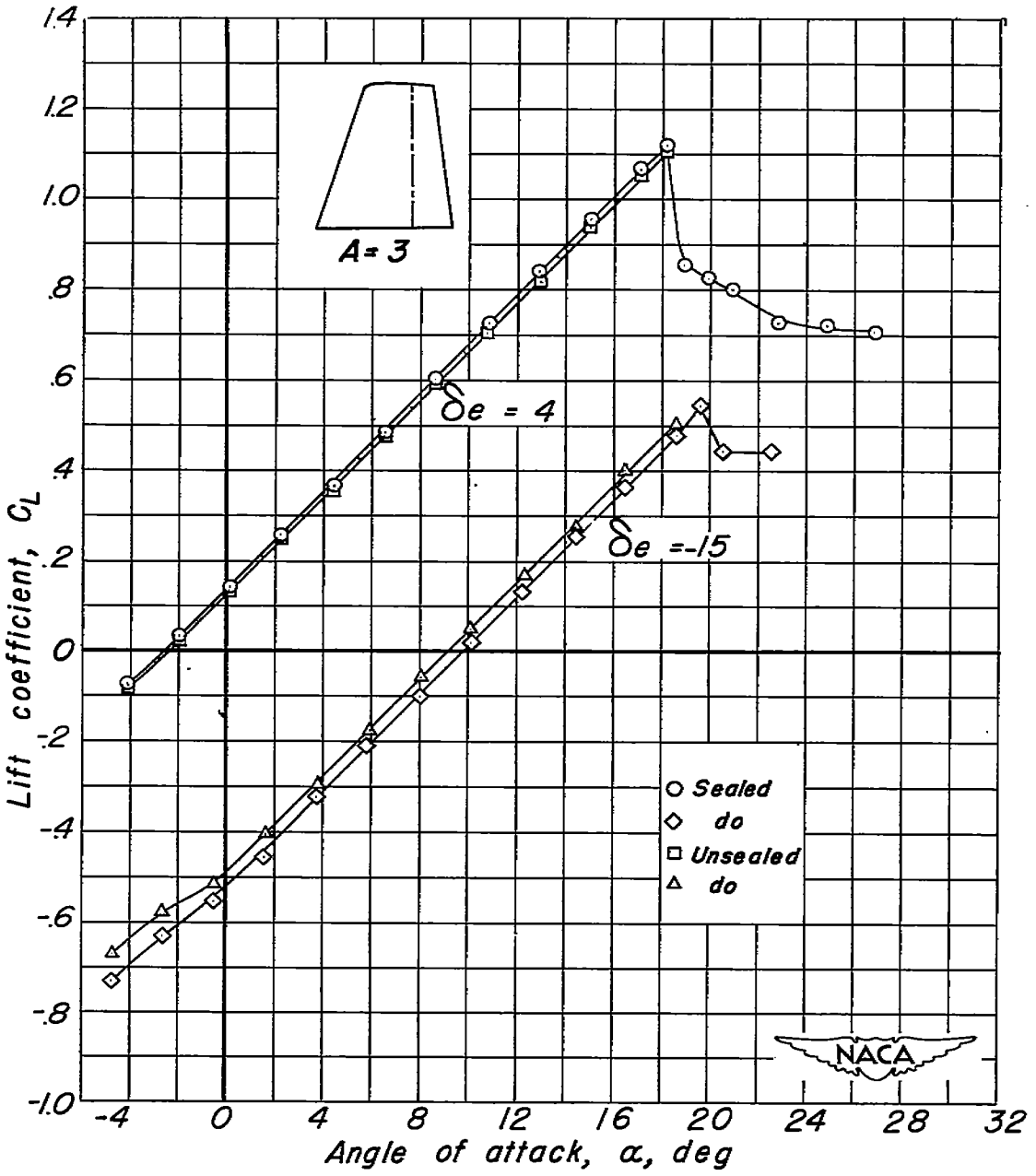

(a) Lift coefficient.

Figure 9.- Comparison of the lift and hinge-moment coefficients with and without elevator seal on the unswept tail. Aspect ratio 3; R, 3.0×10^6.

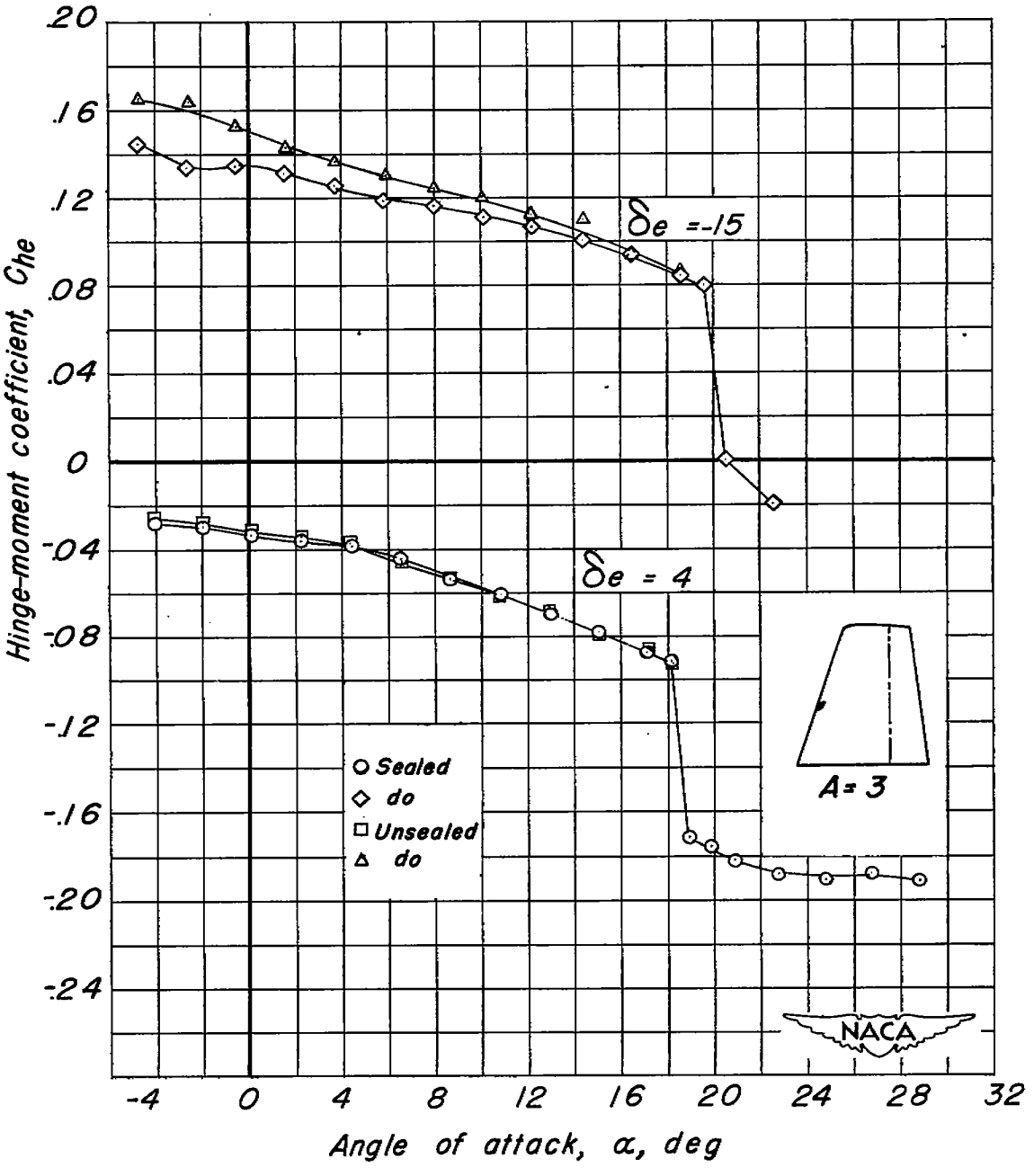

(b) Hinge-moment coefficient.

Figure. 9. —concluded.

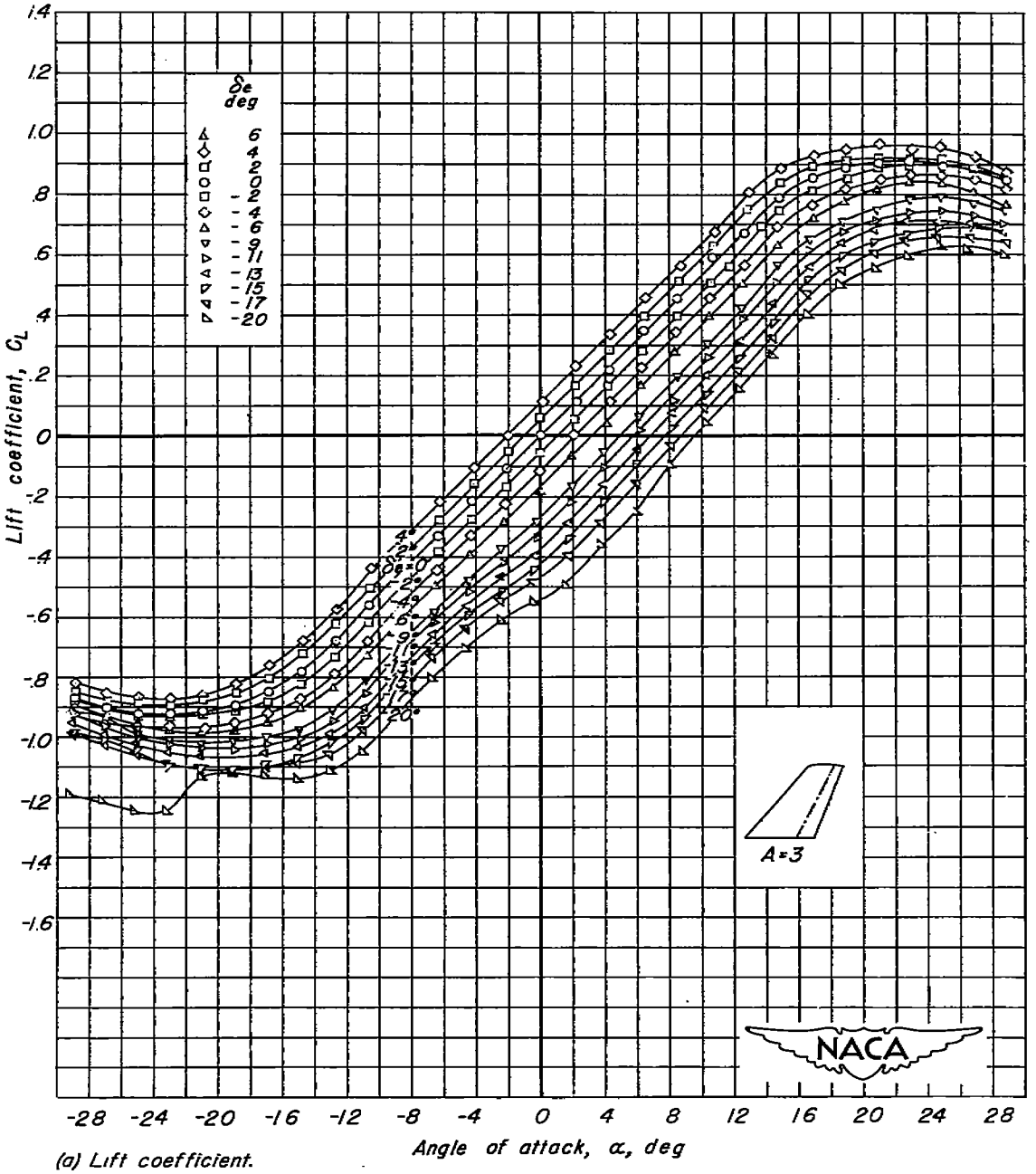

(a) Lift coefficient.

Figure 10.- Lift, hinge-moment, and pitching-moment coefficients of the 35° swept-back tail. Aspect ratio 3; R, 3.0×10⁶.

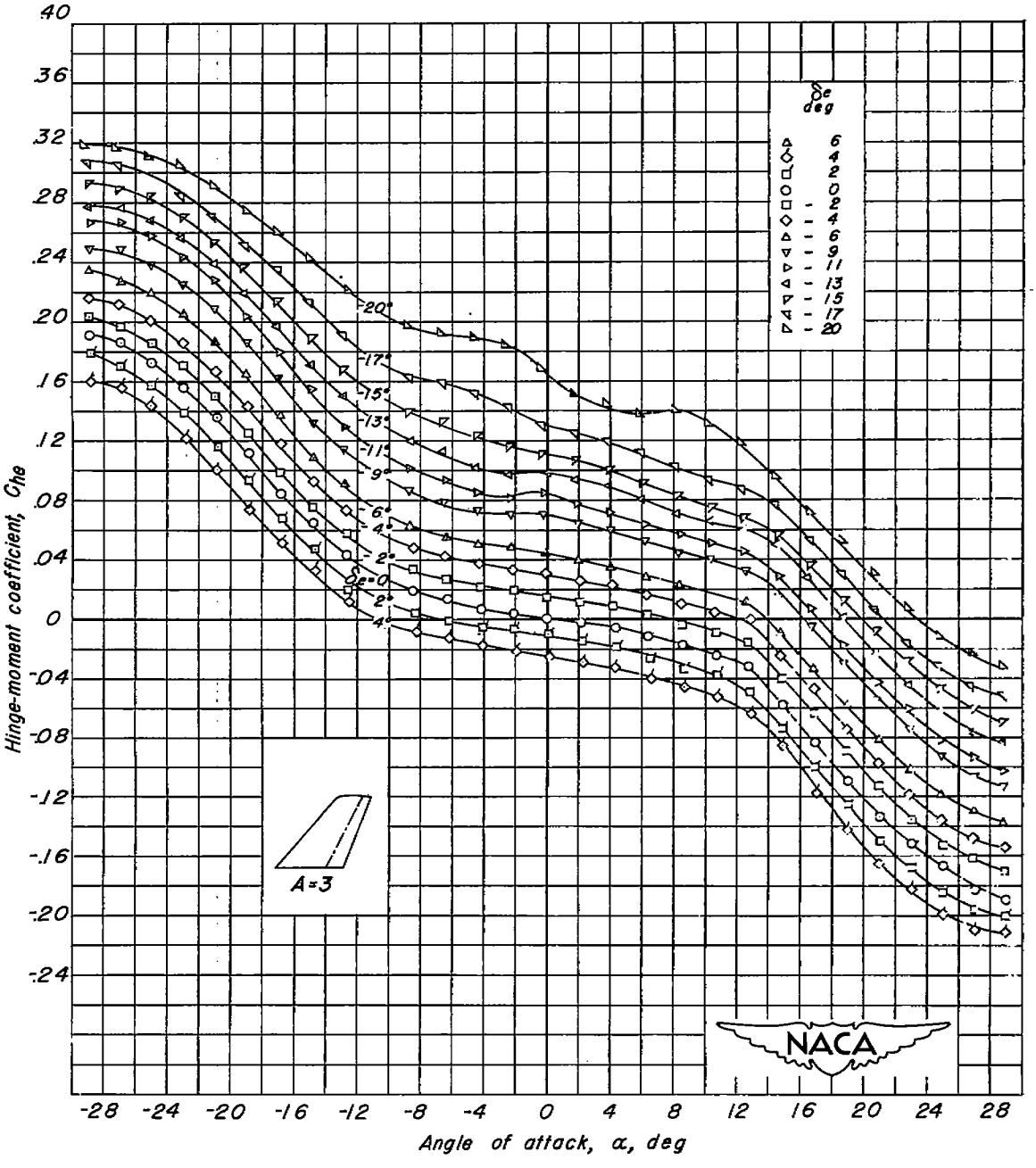

(b) Hinge-moment coefficient.

Figure. 10. — continued.

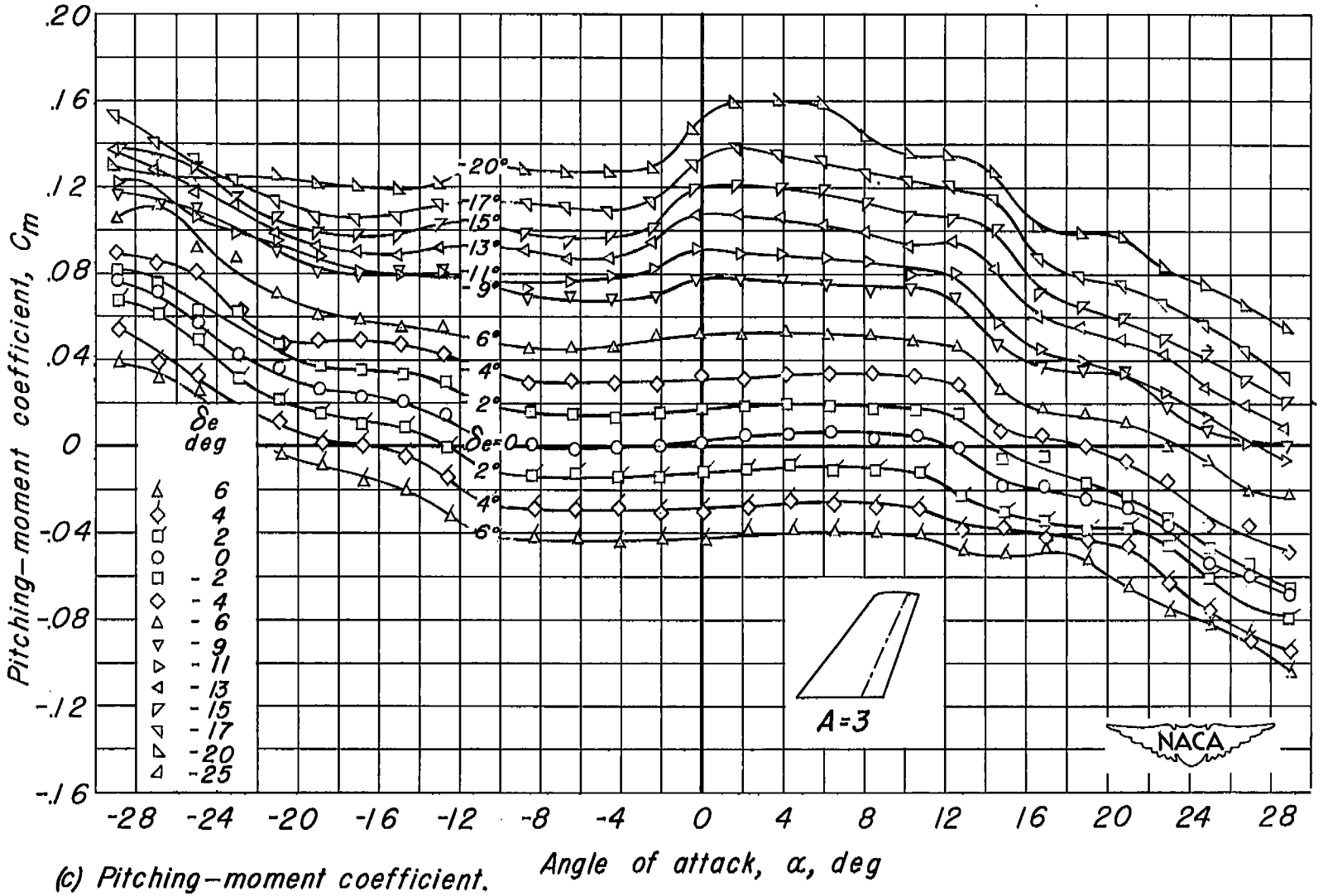

(c) Pitching-moment coefficient.

Figure. 10. —concluded.

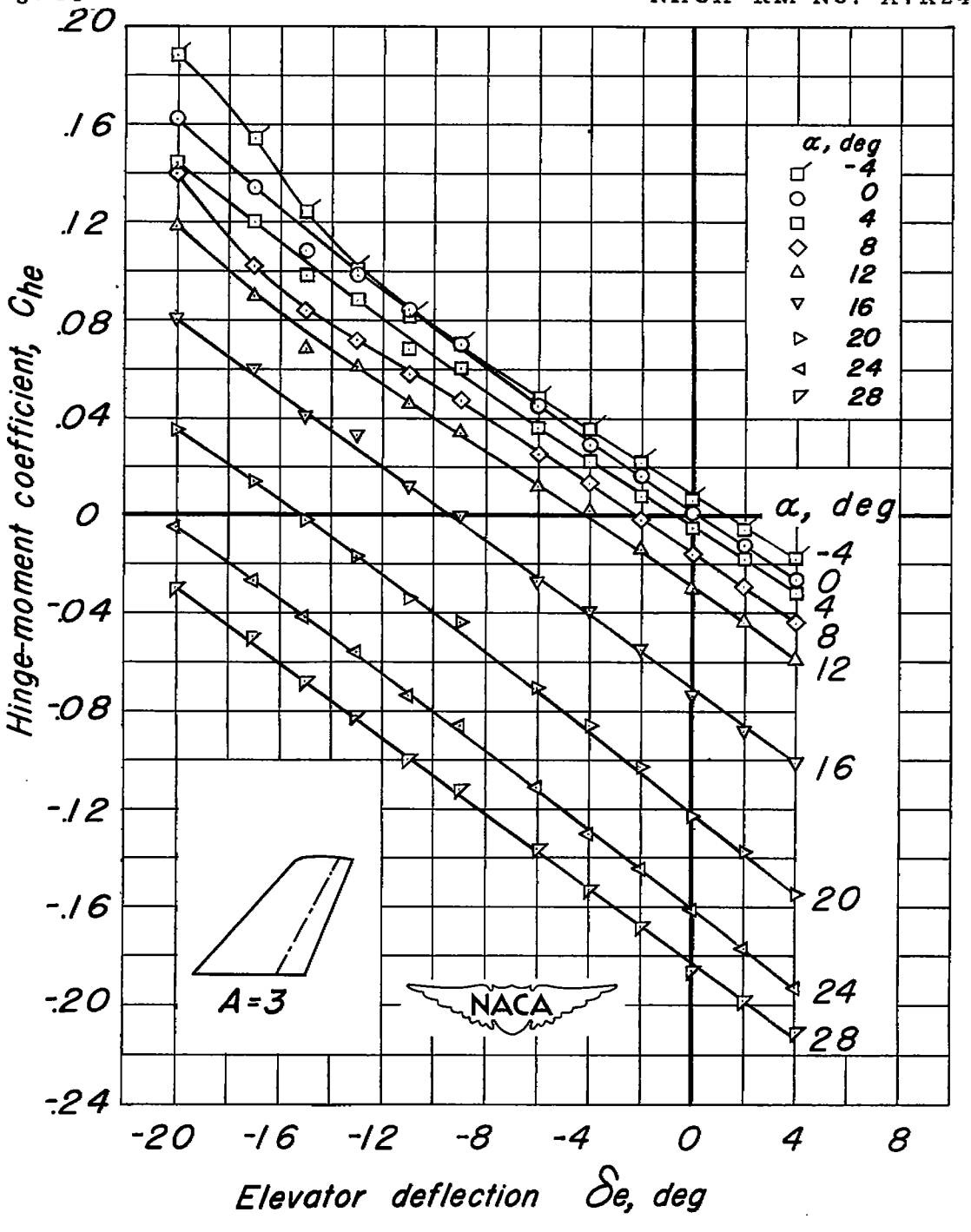

Figure 11.- Variation of hinge-moment coefficients with elevator deflection for various angles of attack of the 35° swept-back tail. Aspect ratio 3; R, 3.0 x 10⁶.

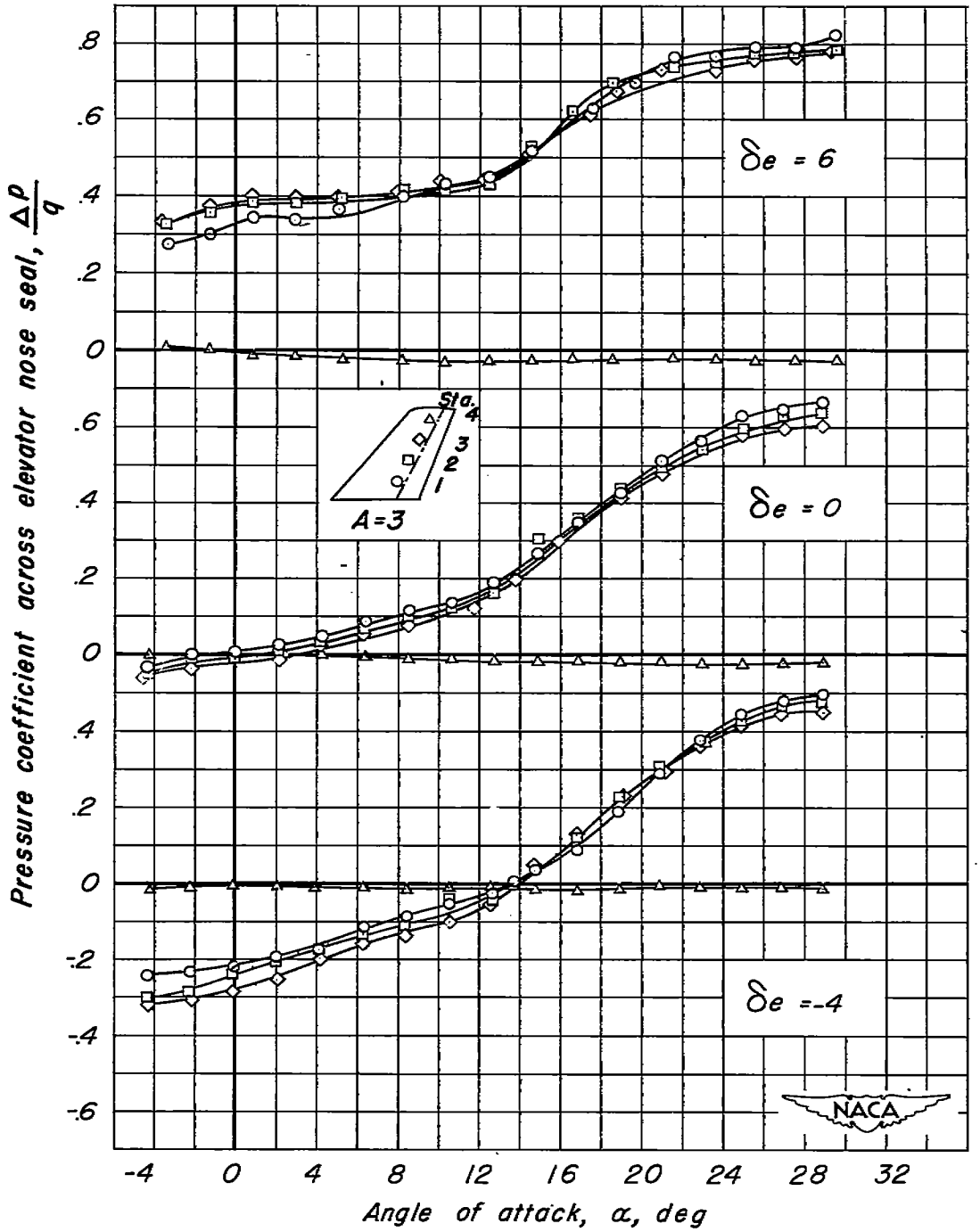

(a) $\delta_e = 6, 0, -4.$

Figure 12.- Variation of pressure coefficient across elevator nose seal with angle of attack of the 35° swept-back tail. Aspect ratio 3; R, 3.0 x 10⁶.

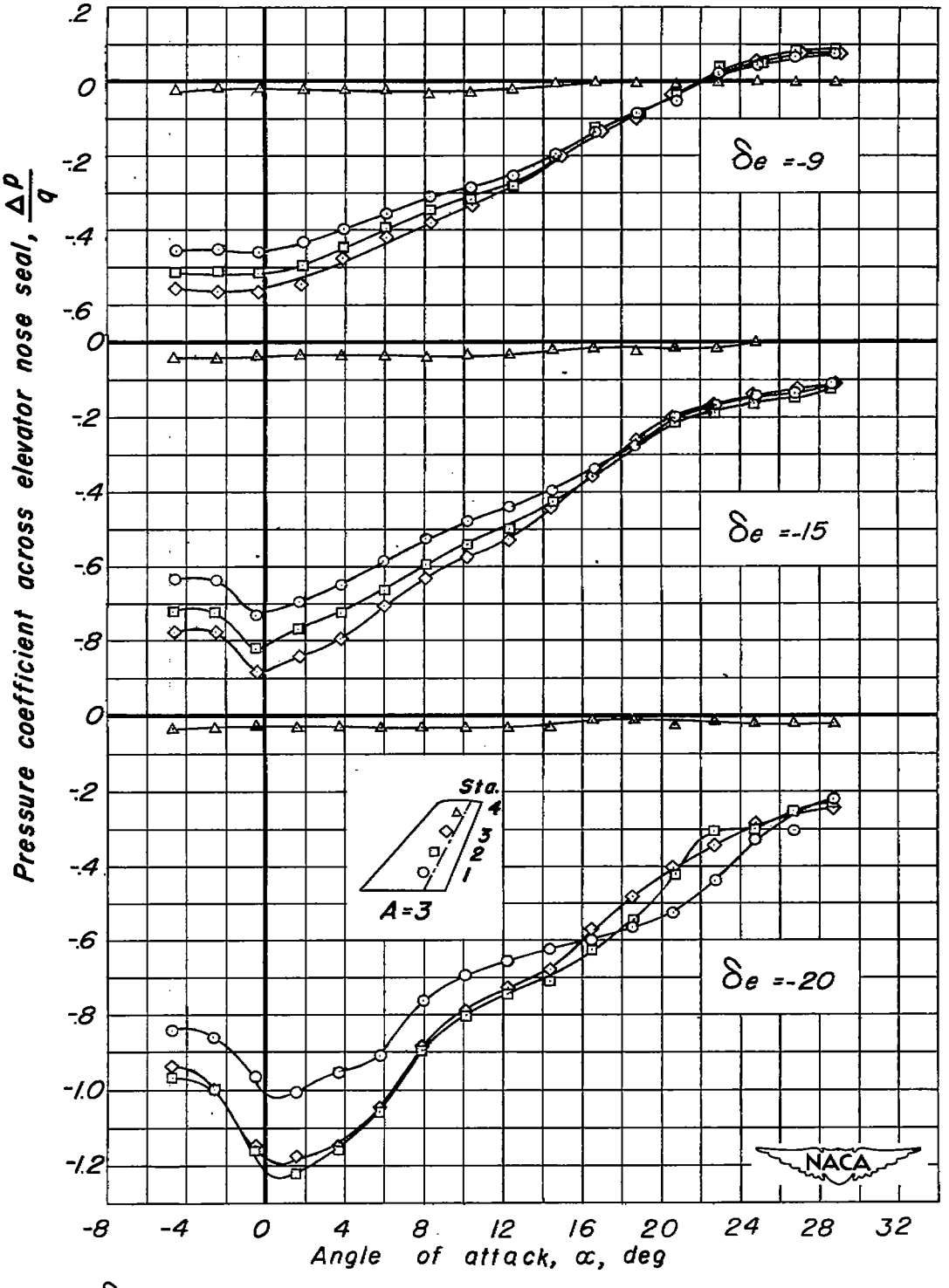

(b) δ_e = -9, -15, -20.

Figure. 12 —concluded.

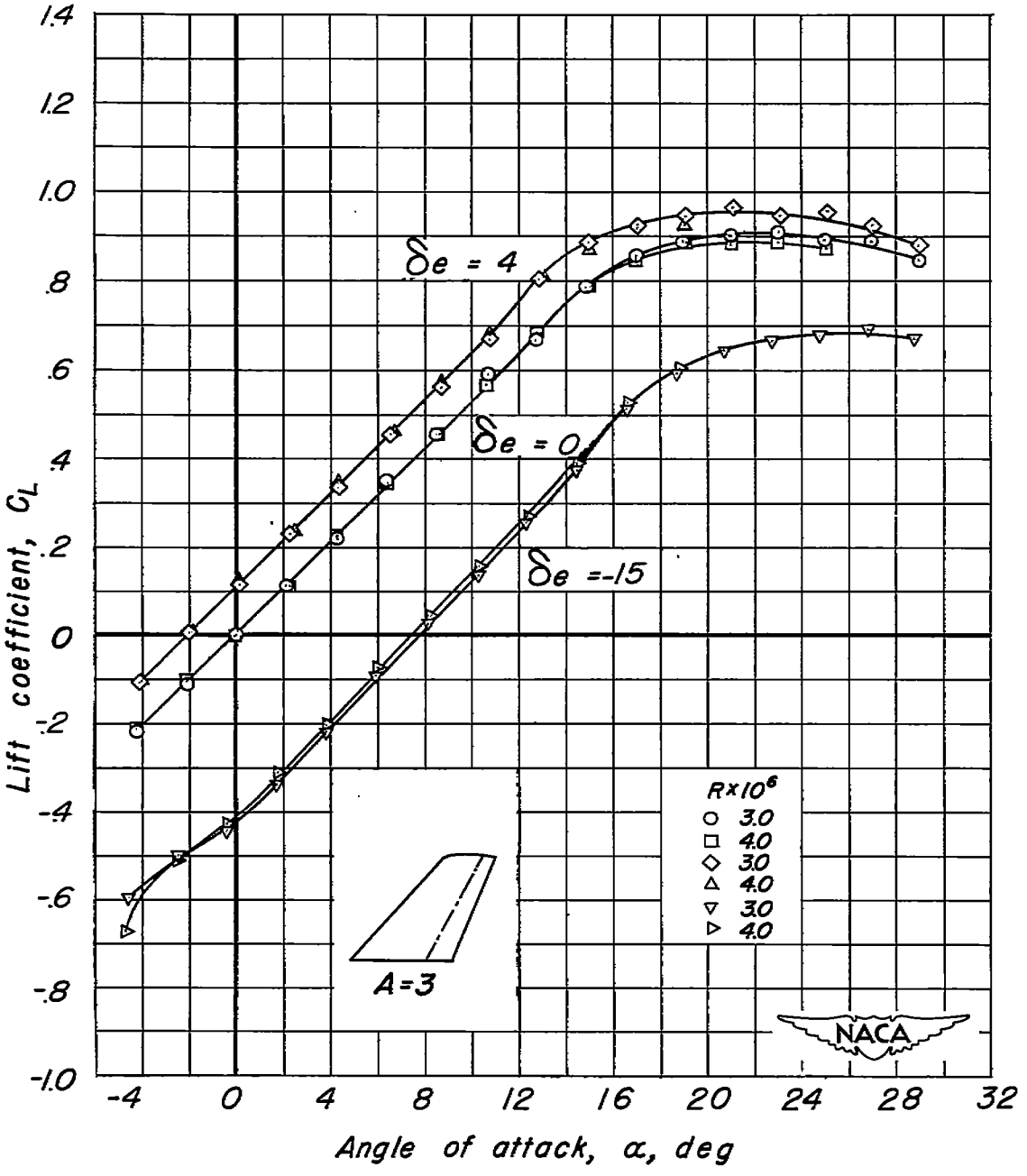

(a) Lift coefficient.

Figure 13.- Comparison of the lift and hinge-moment coefficients at $R=3.0\times10^6$ and 4.0×10^6 for the 35° swept-back tail. Aspect ratio 3.

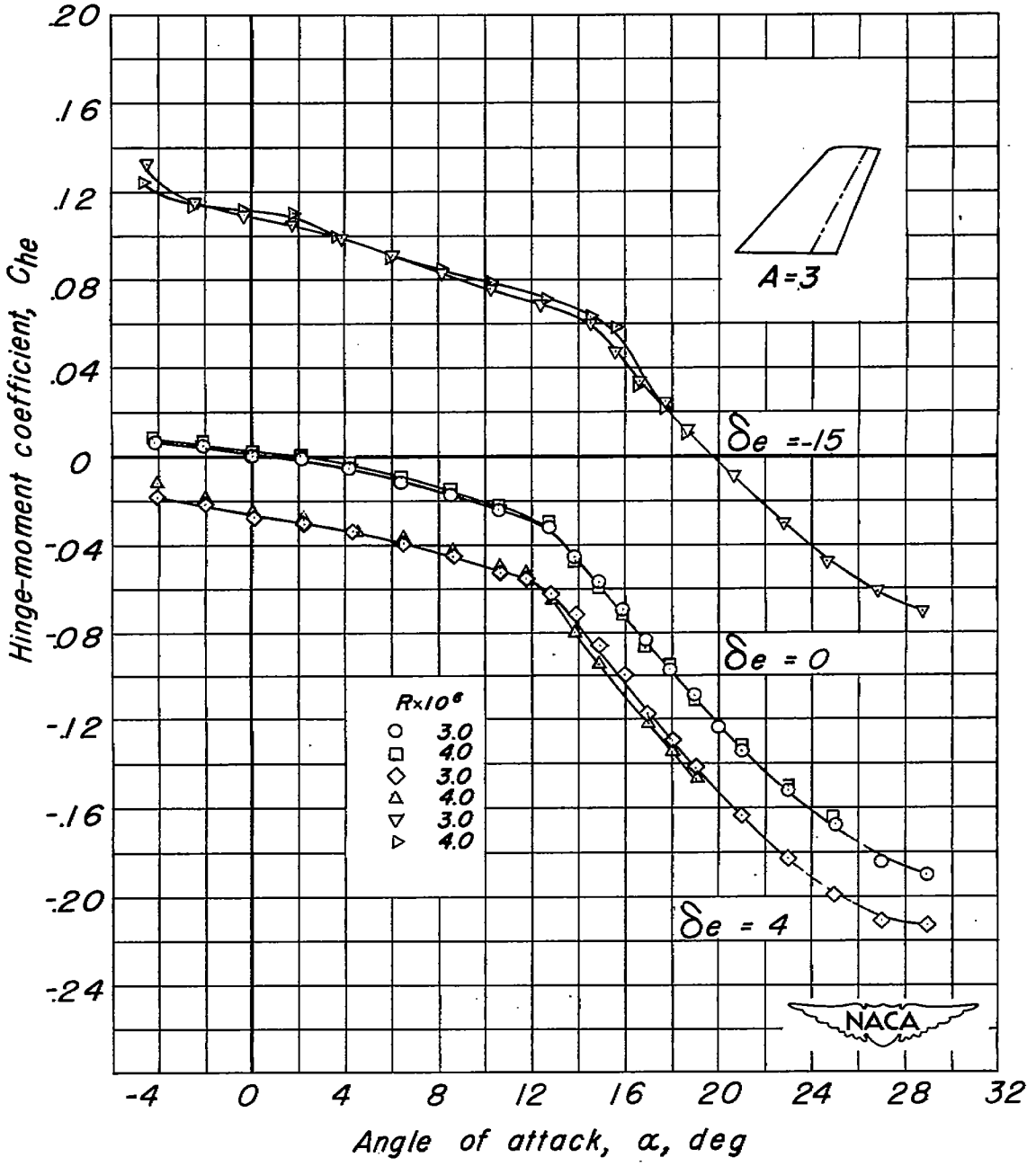

(b) Hinge-moment coefficient.

Figure. 13. —concluded.

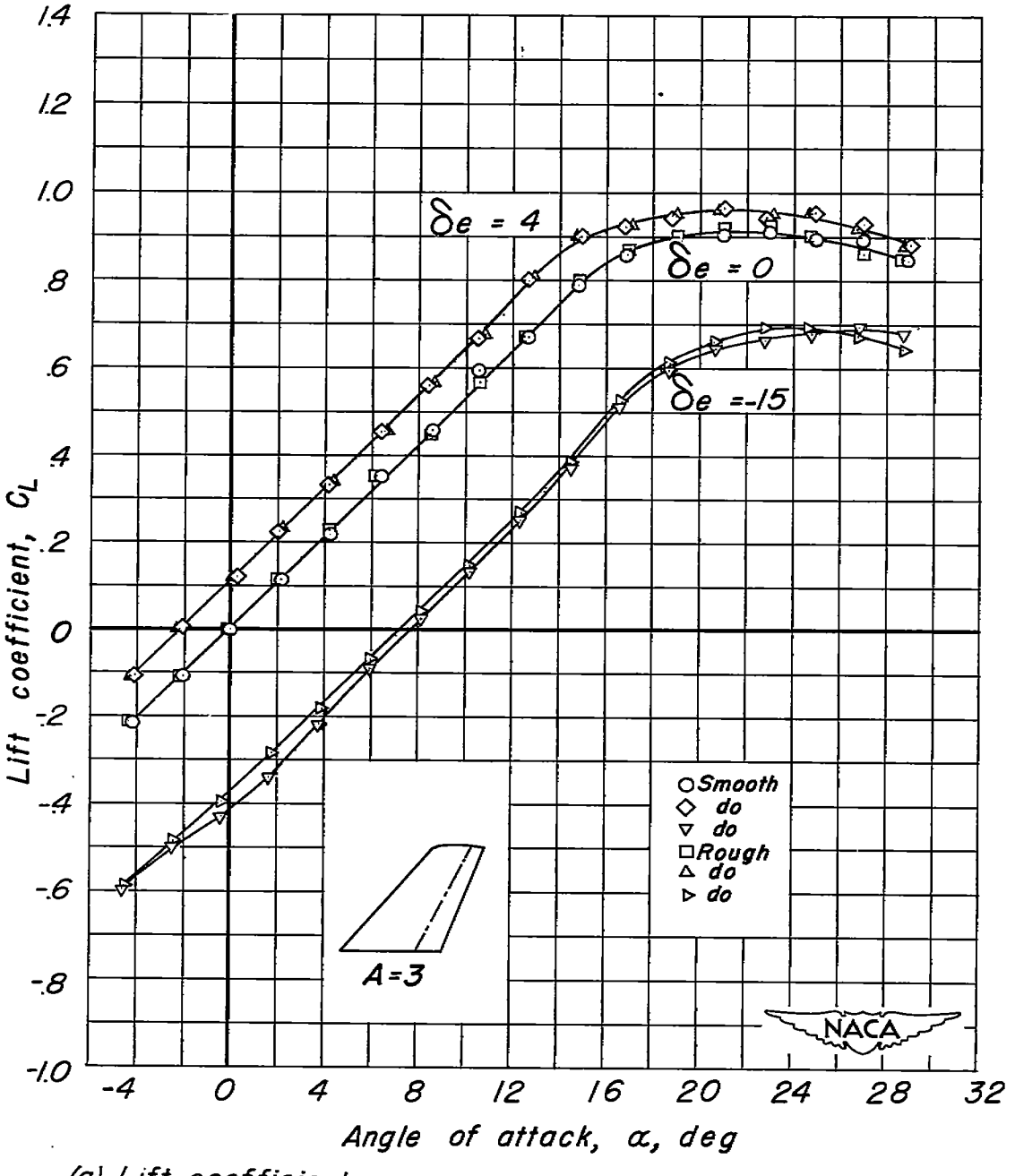

(a) Lift coefficient.

Figure 14.- Comparison of the lift and hinge-moment coefficients of the smooth and rough 35° swept-back tail. Aspect ratio 3; R, 3.0×10^6.

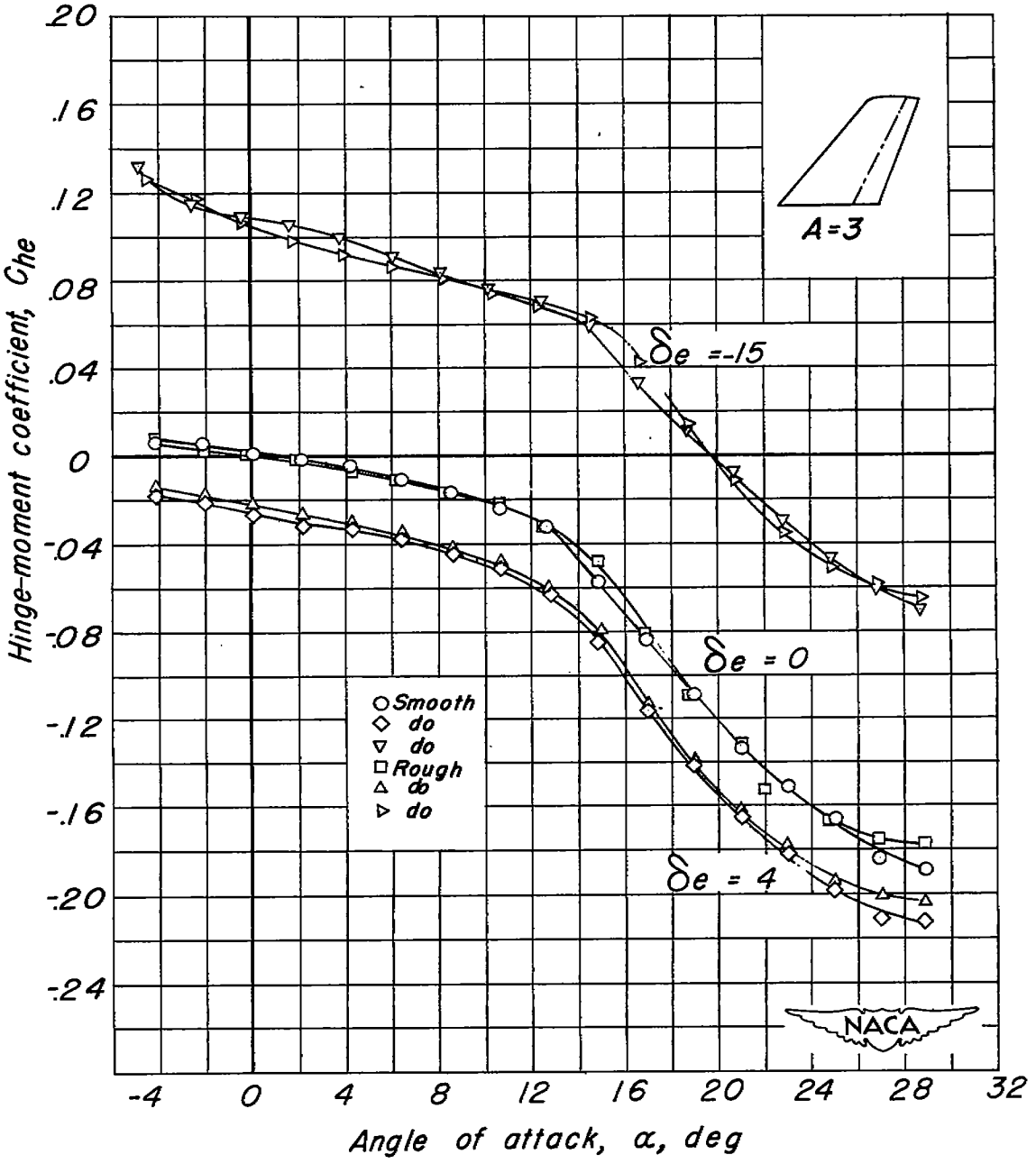

(b) Hinge-moment coefficient.

Figure. 14. —concluded.

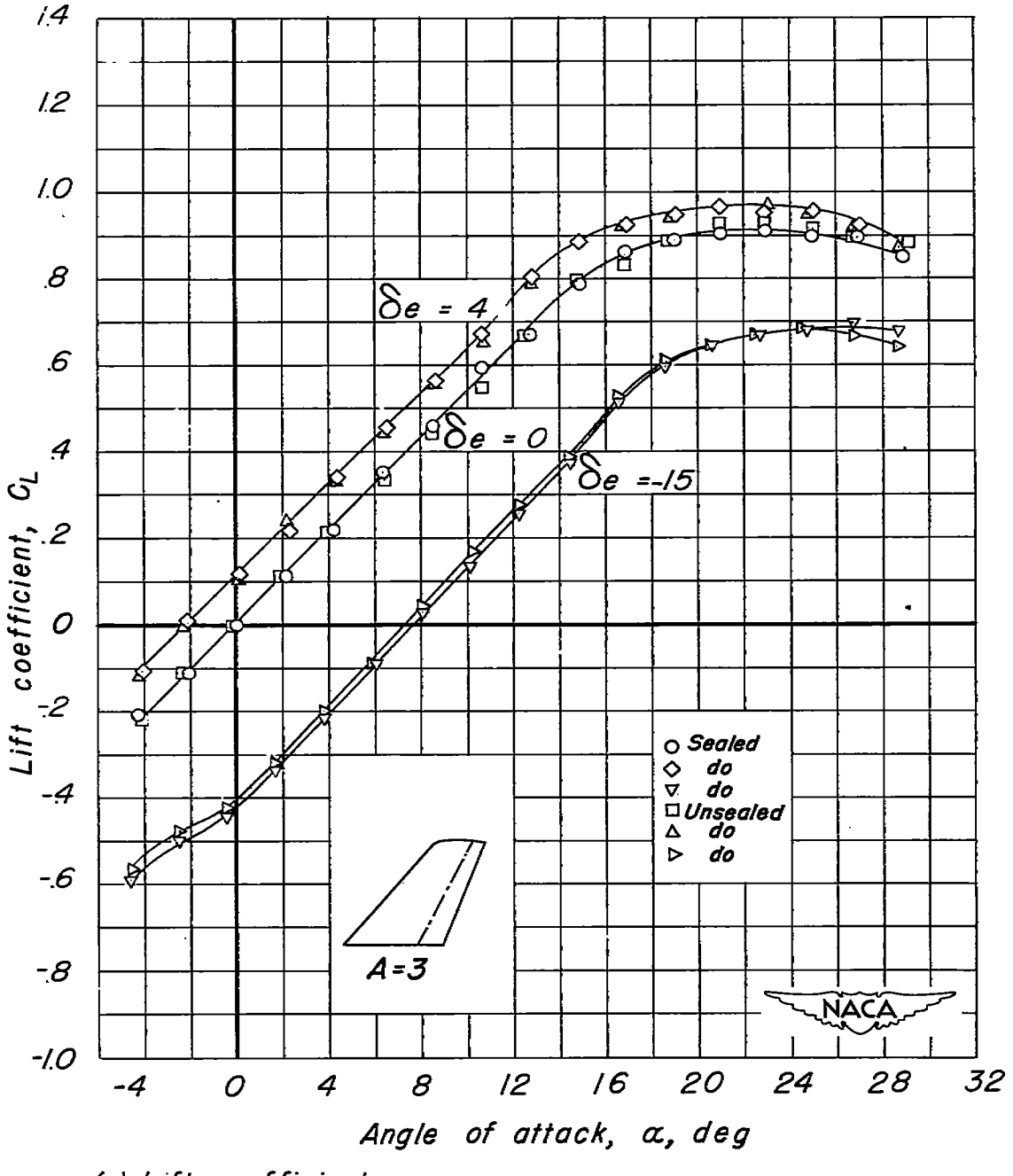

(a) Lift coefficient.

Figure 15.- Comparison of the lift and hinge-moment coefficients with and without elevator seal on the 35° swept-back tail. Aspect ratio 3; R, 3.0 x 10⁶.

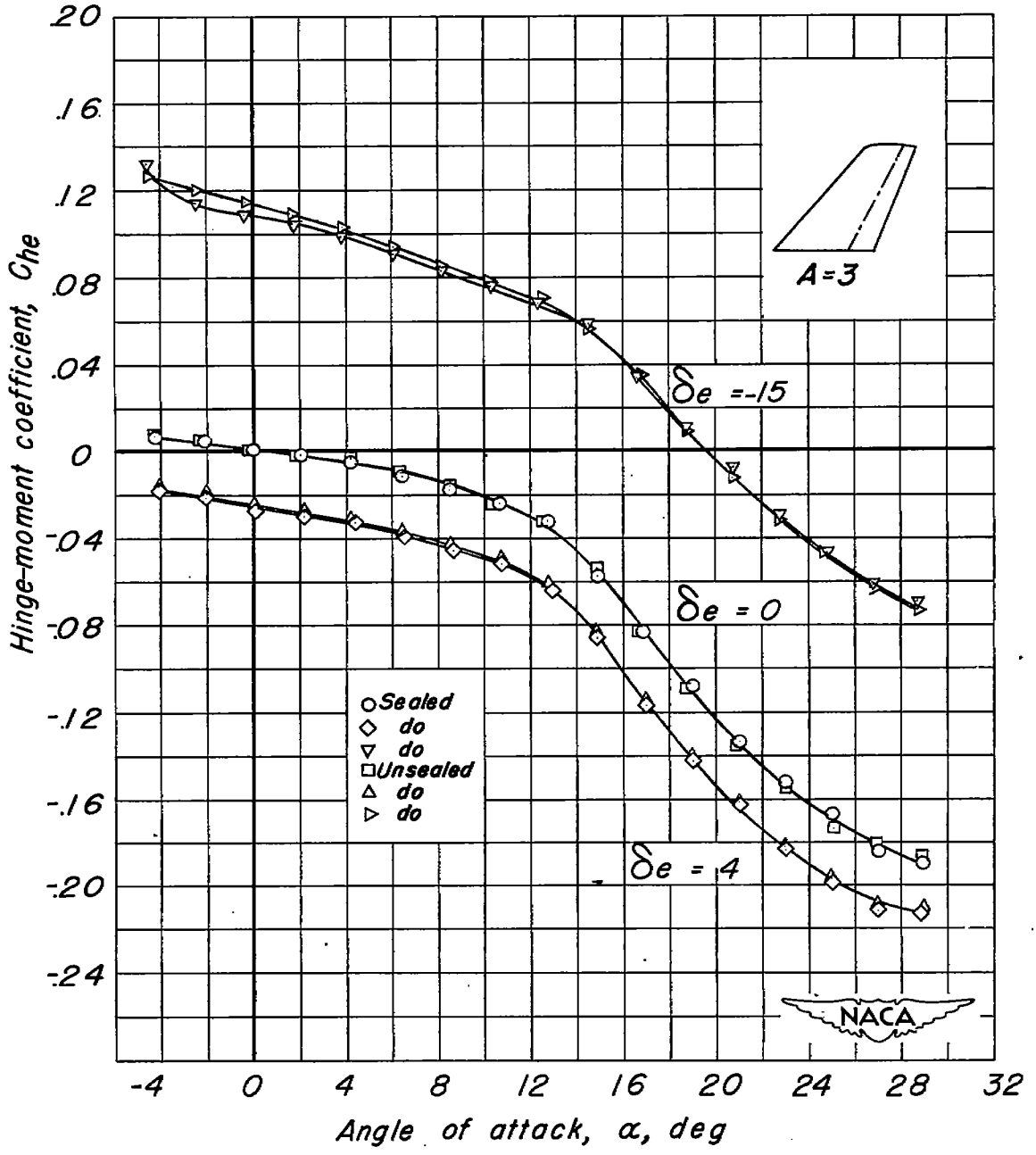

(b) Hinge-moment coefficient.

Figure. 15. —concluded.